3

El Niño/Southern Oscillation and streamflow in the western United States

DANIEL R. CAYAN

U.S. Geological Survey, Climate Research Division Scripps Institution of Oceanography, La Jolla, California 92093-0224, U.S.A.

ROBERT H. WEBB

U.S. Geological Survey, Desert Laboratory 1675 W. Anklam Rd., Tucson, Arizona 85745, U.S.A.

Abstract

The response of western United States precipitation, snow water content (SWC), and streamflow to El Niño/Southern Oscillation (ENSO) conditions was examined. Analyses were conducted over time scales from a season to a day, using several decades of instrumental records. The results reinforce and clarify the association with precipitation found in previous studies. Seasonal SWC and streamflow tend to be enhanced in the southwestern United States and diminished in the northwestern United States during the mature Northern Hemisphere winter El Nino phase of ENSO. Opposite behavior occurs during the La Nina phase of ENSO.

An analysis of the behavior of daily precipitation during the El Nino, La Nina, and 'other year' phases of ENSO reveals further detail. Here we examined differences in the distribution of daily precipitation, stratified seasonally, over the Yellowstone River, Montana, representing the interior northwestern United States, and the Salt River, Arizona, representing the southwestern United States. Both the frequency and the amount of precipitation exhibited significant, opposite-tending changes during the warm and cool phases of ENSO. At Yellowstone River, there is a noticeable reduction in the amount and the frequency of occurrence of early winter daily precipitation during El Nino and a corresponding increase during La Nina. At Salt River, there is an increase in the amount and particularly the frequency of early winter and late winter/spring precipitation during El Niño and a corresponding decrease during La Nina.

Typical precipitation-producing atmospheric circulations were examined via composites of Northern Hemisphere 700-mb height associated with days having

appreciable precipitation during El Niño vs. La Nina. A consistent picture emerged for Yellowstone and Salt River. While the synoptic-scale anomaly features of El Niño and La Niña daily precipitation were similar during early winter, there were significant differences during late winter/spring. The El Nino pattern shows evidence of a North Pacific basinwide activated storm track imbedded in strong westerlies. The La Niña pattern appears to be more confined to the eastern North Pacific and regions downstream, with a high to the west in the Gulf of Alaska vicinity and a low (often a cutoff low) along the West Coast.

Flood frequency in the southwestern United States is affected by ENSO, but this effect varies spatially, and the climatic causes are unclear. The largest floods in Arizona have occurred during El Nino years, and certain rivers, such as the Santa Cruz River, have an increased flood frequency during or just after El Nino conditions. However, rivers strongly affected by winter storms and snowmelt, such as the Salt River, may be affected more by storms occurring during years other than ENSO. One reason for the complexity of the response of streams to ENSO is that there are at least three different types of storms which generate floods. These include frontal systems, which occur predominantly in winter, and monsoonal storms and dissipating tropical cyclones, which usually occur in summer or early fall. The types of storms that generate flooding are affected by El Nino conditions, but the effects are not consistent among El Nino years. Thus, the occurrence of El Niño conditions alone is not sufficient to explain increased flood frequency; instead, large floods appear to occur during a small subset of years associated with El Niño conditions.

Introduction

Since the El Niño/Southern Oscillation (ENSO) is probably the foremost climate variability feature in the short time scale range of a season to a few years, we wish to investigate associated variability in surface hydrological conditions. In this case we focus on behavior of the water supply and flooding over the western United States.

Several previous studies have examined the effect of ENSO on seasonal climate in the extratropics. Specifically, these have shown that during the warm 'mature' phase of El Niño, cool-season precipitation tends to be less in the Pacific Northwest and greater in the southwestern United States (Douglas and Englehart 1981; Ropelewski and Halpert 1986; Andrade and Sellers 1988; Cayan and Peterson 1989; Redmond and Koch 1991.) Previous studies (e.g., Kiladis and Diaz 1989) have shown that opposite effects tend to occur in most regions, including western North America, during the cold phase of the tropical Pacific, which is often called La Niña. While they are weaker than ENSO-related effects elsewhere on the globe (Ropelewski and Halpert 1986), these western North America connections are statistically significant (Kiladis and Diaz 1989), and are as strong as other prominent large-scale climate associations in the Northern Hemisphere (Cayan and Peterson 1989). Furthermore, these connections may have a practical

value in that the low frequency nature of tropical ENSO variations introduces a time lead, permitting some predictive capability at a season or more in advance. Finally, despite the problems in statistical reliability, the great impact of ENSO connections during certain events, such as 1983, cannot be ignored.

The reason for the ENSO connection lies in the atmospheric circulation, where upper level wind shifts change the track and intensity of storms. Theoretical studies suggest that these are responses to anomalous heating in the tropics, induced by the altered sea surface temperatures and lower level wind convergence. During the winter mature phase of El Nino, a tendency for a stronger, more persistent high pressure ridge over western Canada is symptomatic of fewer storms in the Pacific Northwest, and a diversion of these storms into the Alaskan coast. A tendency for low pressure activity in the south also occurs during these episodes, leading to heavier than normal precipitation in the southwestern United States. Unfortunately, the connection is complicated in that there is not a unique pattern associated with El Nino in the North Pacific/North American sector, and work by Fu et al. (1986) and Livezey and Mo (1987) suggest that two or three patterns may be possible.

The intent of this paper is to examine closer the relationship of precipitation, snowpack, streamflow, and flood events in the western United States to ENSO. We examine the El Nino influence on the surface hydrology in terms of both seasonal and shorter term daily fluctuations, including extreme events represented by floods in the southwestern United States.

Data

Data employed in this study include instrumental records of atmospheric, surface meteorological, streamflow, and snow water content variables. Time scales employed include daily through seasonal averaged data.

The atmospheric circulation is represented by twice-daily analyses of the 700-mb height over the Northern Hemisphere, gridded onto a 5°C latitude-longitude grid, available since 1947. Anomalies were computed from long-term means of the daily average (OZ and 12Z analyses averaged together) over the 30-yr period 1950–1979. The height of the 700-mb pressure surface, which is typically 3 km aloft, provides a good representation of the mid-tropospheric circulation. A longer record of the atmospheric circulation is provided by Northern Hemisphere sea-level pressure (SLP) analyses which are available in monthly mean form beginning in 1899 (Trenberth and Paolino 1980). When used here, SLP anomalies were computed from the long-term mean over the entire record (1899–1988).

The state of the tropical Pacific is represented by the Southern Oscillation Index (SOI), an index of the surface pressure gradient across the tropical Pacific basin. When SOI is negative, the tropical Pacific is usually in its warm (El Nino) state, and when it is positive, the tropical Pacific is usually in its cool ('La Niña') state. The form of the SOI used here is the standardized anomaly difference

between Tahiti and Darwin as employed by the NOAA Climate Analysis Center (Ropelewski and Jones 1987). Seasonal average values are employed here. Also, to group events into different year types, years of El Nino and La Nina, as identified by Quinn et al. (1987) and Rasmusson and Carpenter (1982) are listed in Table 3.1.

To explore further relationships to atmospheric circulation over the central North Pacific, abbreviated CNP, a sea-level pressure (SLP) index, was constructed (Cayan and Peterson 1989). This is the average of SLP anomalies over a broad region of the central North Pacific: 35–55°N and 170°E–150°W. To characterize the magnitude of CNP during strong and weak central North Pacific low cases, the average CNP for the 25 strong CNP cases is less than −7 mb, while it exceeds +7 mb for the 25 weak cases. In both composites, the strongest anomaly center is found at about (50°N, 165°W). This index is similar to the well-known Pacific-North American (PNA) index, the most important winter

Table 3.1 *El* Nino and La Nina years[a] .

El Niño	La Niña
1901	1904
1903	1907
1906	1909
1912	1917
1915	1921
1919	1925
1924	1929
1926	1932
1931	1939
1933	1943
1940	1950
1941	1955
1942	1965
1947	1971
1952	1974
1954	1976
1958	1989
1964	
1966	
1970	
1973	
1977	
1978	
1983	

"Years listed are water years (October of previous calendar year through September of listed calender year).

circulation mode in the central North Pacific (Davis 1978; Barnston and Livezey 1987; Namias et al. 1988). The SLP data for deriving CNP is available since 1899 while the upper level geopotential height data to derive the PNA index does not begin until 1947. This simple index is well related to PNA in the cool months; correlations between CNP and PNA are −0.69, −0.90, and −0.75 in fall, winter, and spring (Cayan and Peterson 1989).

The streams employed were selected to provide reliable records over the longest possible period. Monthly average streamflow from 61 stations over western North America and Hawaii were obtained from the U.S. Geological Survey and Canadian archives (U.S. Department of Interior 1975). The 61 streams include 52 from the western coterminous United States, 3 from British Columbia, 4 from Alaska, and 2 from Hawaii. Most of the streamflow records begin between 1900 and the 1930s; the longest series, Spokane River at Spokane, Washington, begins in 1891. Most of the streams employed have records updated through 1986, and several have records through 1988. These latter include the Yellowstone River, Corwin Springs, Montana, and the Salt River, Roosevelt, Arizona, which are used for more detailed analyses with ENSO.

For several decades, the USDA Soil Conservation Service (SCS) has archived snow observations at several hundred mountain snow courses in the western United States. Snow water content (SWC) is affected by both accumulation and ablation of snow, but at many locations in the West, there is maximum SWC in spring near the beginning of April. This study employs a set of approximately 400 SWC records for the period 1950 to 1989. Snow courses are usually located at relatively high elevation sites, but because of the variety of topography in the West, a broad range of elevations are represented, from about 500m to over 3000 m. Many snow courses have observations taken at the beginning and sometimes the middle of each of the months with substantial snow cover from January through May. For purposes of this study, we use only those taken on the beginning of the month.

To examine the ENSO connection to individual watersheds, daily precipitation at two individual river basins was utilized. These basins, representing the northwestern United States and the southwestern United States were the Yellowstone River upstream of the Corwin Springs, Montana gauge, and the Salt River, upstream of the Roosevelt, Arizona gauge. Basin average precipitation for Salt River and Yellowstone River was constructed from a weighted average of precipitation from six stations within or nearby the watershed. The stations (Table 3.2) were selected because they had several decades of record and showed no apparent artificially caused discontinuities or trends. In deriving the basin average precipitation, a scheme was used to weigh contributions from stations which contained sometimes quite different precipitation statistics. The idea of this scheme was to average the standardized precipitation anomaly, multiply this standardized anomaly times the 'overall' basin standard deviation, and add this anomaly to the 'overall' basin mean for that day. On days when all stations recorded zero precipitation, the basin average precipitation was zero. On days

Table 3.2 *Precipitation stations for individual watersheds*

Station	Elevation (m)	Period
Yellowstone River		
Hebgen Dam, Montana	1973	1948–1989
Island Park, Idaho	1912	1937–1989
Lake Yellowstone, Wyoming	2369	1948–1989
Tower Falls, Wyoming	1912	1948–1989
West Yellowstone, Montana	2030	1924–1989
Yellowstone Park, Wyoming	1890	1948–1989
Salt River		
Buckeye, Arizona	265	1893–1989
Clifton, Arizona	1055	1893–1989
McNary, Arizona	2231	1933–1989
Miami, Arizona	1085	1914–1989
Roosevelt 1 WNW, Arizona	674	1905–1989
Springerville, Arizona	2152	1911–1989

when at least one station recorded precipitation, the basin average precipitation was constructed by averaging the standardized precipitation anomaly times an 'overall' basin standard deviation, plus the average daily precipitation for the basin. The overall basin standard deviation, σ_T, was computed using

$$\sigma_T \left[\frac{1}{n} \sum_{i=1} \sigma_i^2 \right]^{1/2}$$

where σ_i^2 is the daily variance at station i. The basin average precipitation was equal to the mean of the daily precipitation at the n stations; n ranged from 3 to 6 stations. To reduce sampling variations of the daily means and standard deviations from finite record estimations, they were smoothed using a 15-d Gaussian filter (the smoothed standard deviation was computed from the smoothed daily variance).

To examine the broad-scale precipitation during individual events, gridded daily precipitation over the coterminous United States (Roads and Maisel 1991) was employed. This set was constructed from 831 stations from the United States cooperative station network, and provided data from 1950 through 1988. The stations, a subset of the National Climatic Data Center United States Historical Climatology Network (Quinlan et al. 1987), were selected because they were relatively insulated from urban effects and had a nearly complete record over the 1950–1988 period. The station precipitation was transformed to a 2.5° grid by averaging all nonmissing daily station values contained within the 2.5° latitude by 2.5° longitude region of each grid point. Note that for the present purpose, these data are used to discover the *qualitative* nature of the spatial distribution of precipitation associated with certain types of events.

ENSO vs. seasonal hydrological variations

Both **SWC** and streamflow are important components of the surface hydrology and the water supply. They are cumulative measures of the surface climate, responding to behavior over the wet season in the western United States. Streamflow has the added benefit of providing a spatial average over a watershed. In many respects **SWC** and streamflow are superior to the precipitation in measuring the water supply in the West, since they represent the amount which is available. Streamflow also records flood events, which will be discussed later for southern Arizona watersheds. **Cross** correlations between seasonal precipitation, **SWC,** and streamflow at Yellowstone River and Salt River are shown in Table **3.3.** At Yellowstone River, these components are all correlated at about **0.7** or greater. At the more arid Salt River region, the correlations of November–March precipitation vs. 1 February **SWC** and water year (October–September) streamflow are **0.7** to 0.8, but the correlation with **1** April **SWC** is only about 0.4. The time series of **SWC** and streamflow at the two locations is shown in Figure **3.1,** along with an indication of years of El Niño and La Niña.

A broad-scale effect of ENSO on surface hydrological variations is evident from correlations of seasonal anomalies of SOI with observations of 1 April **SWC** and mean December–August streamflow. The **1** April **SWC** and (December–August) streamflow measures are cumulative seasonal indices representative of several months of climatic activity. To examine behavior concurrent with, and subsequent to the tropical conditions, correlations are calculated using both winter and preceding summer SOI. For comparison with mid-latitude circulation influences, correlations with seasonal **CNP** (winter and the preceding fall) are also presented. Summer **CNP** is not well related to the following winter atmospheric circulation, so this relationship is not shown.

The correlations between SOI and **SWC,** and SOI and streamflow are similar in pattern and magnitude. The'correlation of SOI during summer and winter vs.

Table 3.3. ***Cross correlalions, Nov-Mar precipitation / Feb SWC, / Apr SWC, and water year streamflow***

	1 Feb SWC	1 Apr SWC	Water year streamflow
Yellowstone River			
Nov-Mar Precipitation	0.83	0.71	0.74
1 Feb SWC		0.78	0.78
1 Apr SWC			0.67
Salt River			
Nov-Mar Precipitation	0.66	0.42	0.84
1 Feb SWC		0.25	***0.58***
1 Apr SWC			0.56

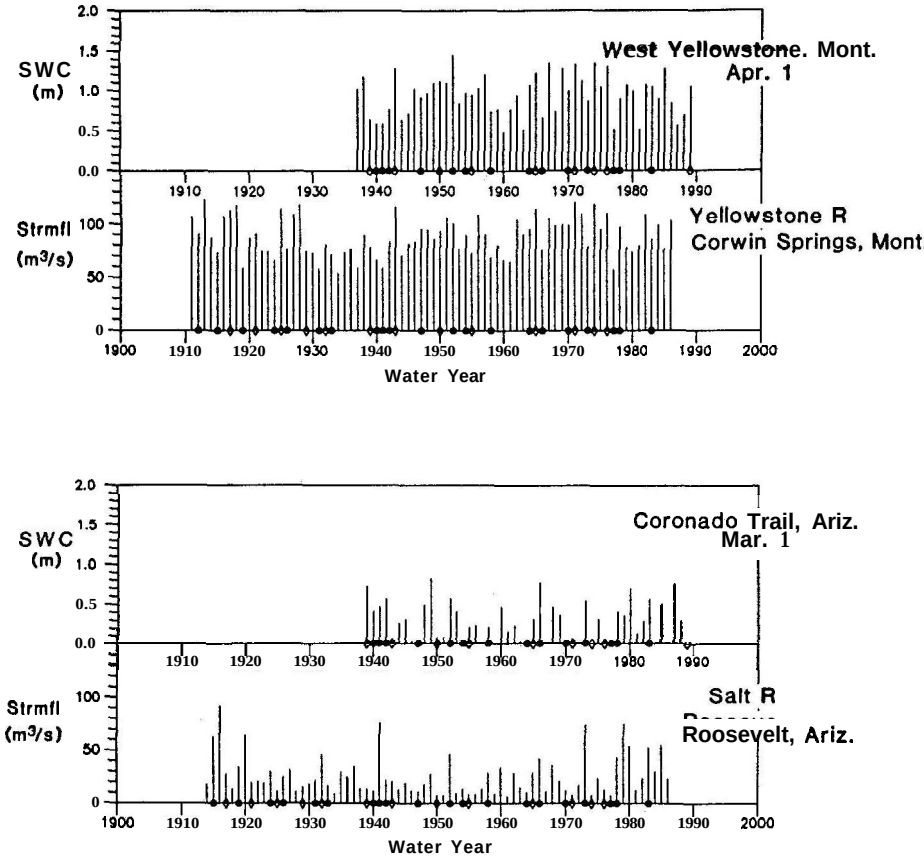

Fig. 3.1 Seasonal snow water content (SWC) and water year mean streamflow, Yellowstone River, Corwin Springs, Montana, and Salt River Roosevelt, Arizona. El Niiio and La Niiia years are denoted by solid circles and open diamonds, respectively.

the subsequent 1 April snow course SWC over the West is shown in Figure 3.2. Corresponding patterns of the correlations between streamflow and SOI are shown in Figure *3.3,* along with comparable patterns for CNP. For SOI, correlations are positive (low SWC during winters of El Niño) over most of the Northwest and negative over a broad .region of the Southwest. Strongest positive correlations, with magnitudes about 0.5, are found in patches over Idaho, Montana, and Wyoming. Maximum negative correlations occur on a broad band over the Southwest, having values of approximately −0.4. Streamflow anomalies in the Southwest from southern California through Arizona and southern Colorado tend to be positive (wet) while those in the Pacific Northwest are negative (dry) during the warm eastern tropical Pacific phase of ENSO. SWC anomalies from available snow courses in the Southwest also tend to be enhanced during El Nino. These relationships are consistent with previous studies of monthly and seasonal precipitation (Kiladis and Diaz 1989). For the moment

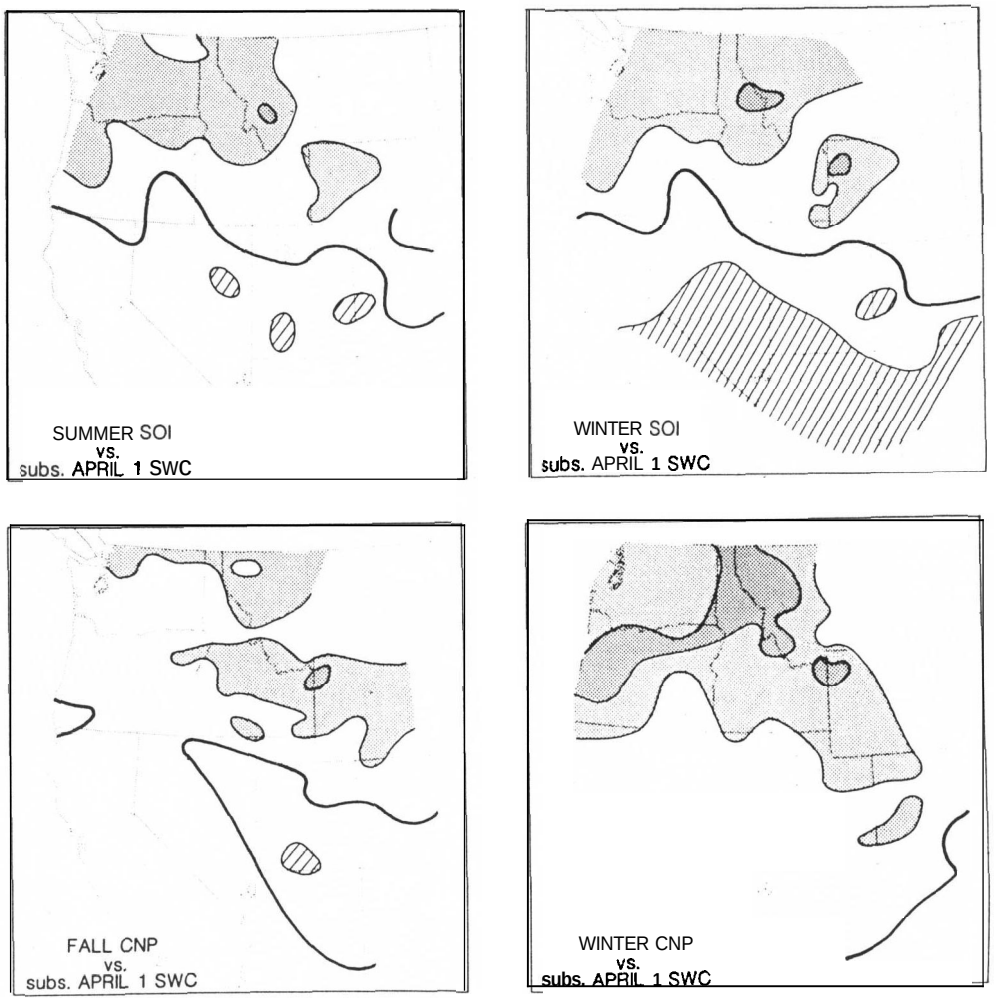

Fig. 3.2 Cross correlations: SOI (above) and CNP (below) vs. subsequent 1 April snow water content (SWC) from western U.S. snow courses. Two seasons SOI and CNP are used: summer or fall preceding, and winter preceding the subsequent (subs.) 1 April SWC. Stippling and hatching indicates correlations $\geqslant 0.3$, 0.5 and $\leqslant -0.3$. -0.5, respectively.

assuming a symmetric relationship between the two ENSO phases, negative SOI (the warm state of the tropical Pacific) is associated with reduced snowpack and streamflow in the Northwest and enhanced snowpack and streamflow in the Southwest. Since the Northwest tends to exhibit warmer winter temperatures (Ropeleski and Halpert 1986) as well as drier than normal conditions during El Niño, the anomalous temperature may also contribute to the reduced snowpack (Redmond and Koch 1991).

While the correlations of SOI vs. SWC and streamflow are somewhat weak (maximum correlations between these seasonal variables are about ± 0.5), there are potentially useful lag relationships. The relatively slow time evolution of the

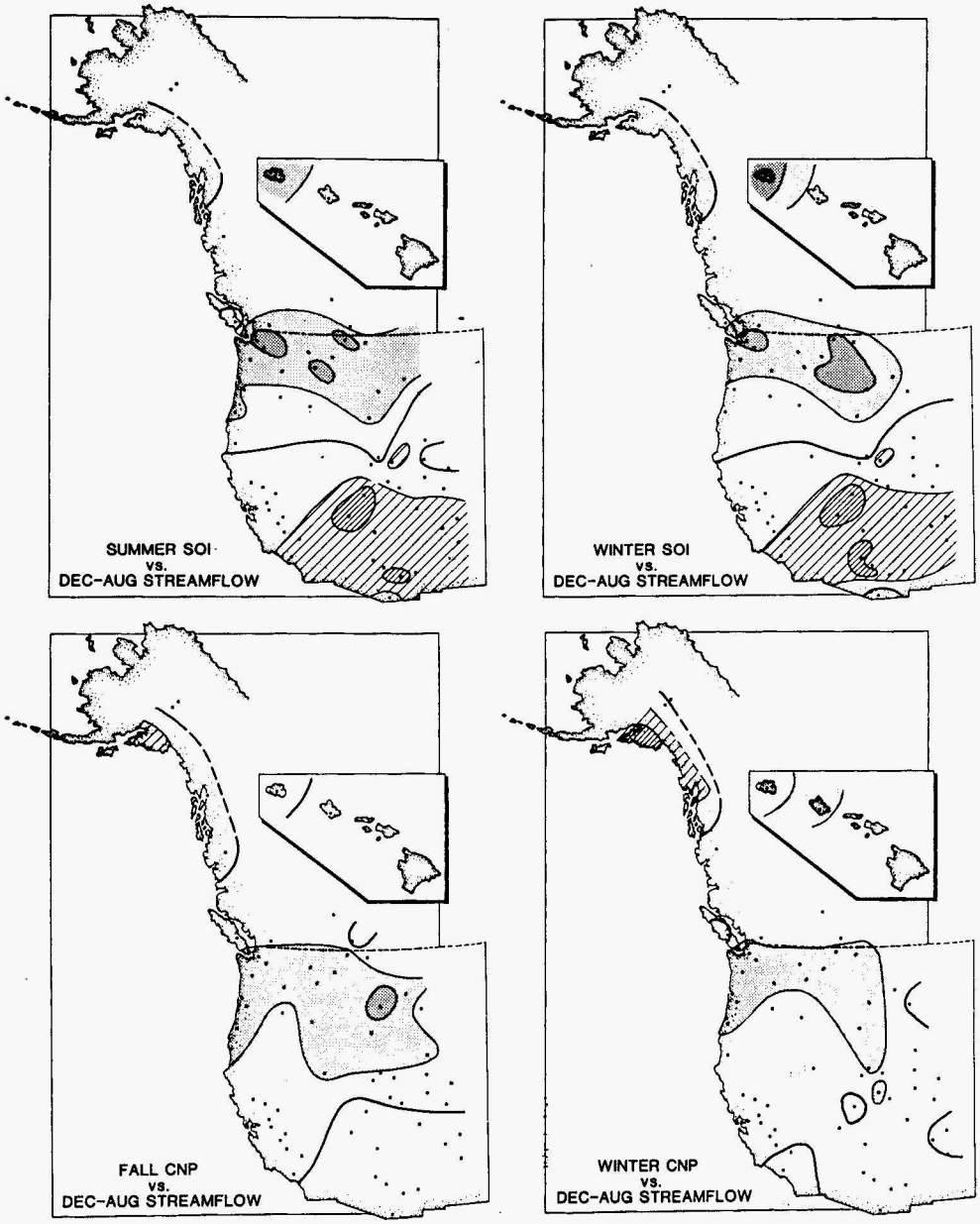

Fig. 3.3 Cross correlations SOI (above) and CNP (below) vs. December–August streamflow of several stream gauges in western North America and Hawaii. Two seasons' SOI and CNP are used; summer or fall preceding, and winter during the December–August streamflow period. Stippling and hatching indicates correlations $\geqslant 0.3$, 0.5 and $\leqslant -0.3$, -0.5, respectively. Dots indicate stream gauge locations. (Modified from Cayan and Peterson, 1989.)

SOI is sufficient to produce the same pattern and nearly the same correlation magnitudes for summer SOI leading as for winter SOI contemporary values with the surface hydrological variables.

The 'mature' winter phase (Rasmusson and Carpenter 1982) of ENSO is associated with low pressure in the central North Pacific in winter. The SOI vs.

streamflow anomaly correlation pattern is similar to that of CNP and PNA, but with two differences. Comparing the SOI and the CNP seasonal correlations, there is a strong similarity with the patterns in the Northwest but not in the Southwest. Correlations with CNP indicate virtually no relationship in the Southwest. The SOI-CNP similarity in the Northwest is not surprising, since, as mentioned, the deep Aleutian low phase of the PNA (the negative phase of the CNP) often occurs during the Northern Hemisphere winter mature phase of El Niño. The connection between SOI and CNP and SWC and streamflow in the Pacific Northwest can be translated in terms of the large scale circulation, the carrying current for North Pacific storms. When the central Pacific low is well developed, North Pacific winter storms tend to be carried northward toward northern British Columbia and Alaska, making that region wet while the northwestern United States is dry. The negative SLP anomalies in the central North Pacific correspond to enhanced storminess south of the Aleutian Islands, and a high pressure anomaly ridge downstream over the Northwest. This flow pattern steers the storm track toward the north into the Alaskan coast instead of into the Pacific coast farther south (see Klein [1957] for storm tracks). In the subtropical North Pacific, there is an anomalous westerly (west-to-east) flow in association with the gradient between the deep central Pacific low to the north and anomalous high pressure to the south. This flow anomaly reduces the trade winds and diminishes precipitation and streamflow on the eastern coastal slopes of the Hawaiian Islands. Conversely, when the Aleutian low is weak, there is a tendency for a more active low to the east in the Gulf of Alaska, so that heavier than normal precipitation, higher SWC, and larger streamflow anomalies tend to occur.

The second difference between SOI and CNP is that along the Alaskan coast, correlations of SOI and streamflow are weaker than with CNP. Nonetheless, the negative correlations with SOI may be meaningful, since Yarnal and Diaz (1986) reported significant correlations between ENSO and coastal Alaskan precipitation. Much of the weakness of this relationship arises from the variability in the longitude of the deepened central North Pacific low during winter that is associated with El Niño (Peterson et al. 1986, Fig. 8). A more westerly position of this trough favors the winter storm track moving into the Alaskan coast, while a more easterly position encourages storms along the West Coast farther to the south. Further insight into the types of Northern Hemisphere circulation patterns that appear with ENSO is provided by Fu et al. (1986) and Livezey and Mo (1987) who suggest that the configuration of tropical Pacific heating may help to determine the pattern of extratropical response.

It is noteworthy that parts of the western United States are ***not*** significantly correlated to either SOI or CNP. Concerning the deep Aleutian Low phase of SOI (warm equatorial Pacific) and CNP, the relative weakness of the southern portion of the teleconnection downstream over the West Coast means that the tendency for high pressure (lack of storminess) is not very reliable. Hence, there **is** not **a** strong CNP relationship over California and the Southwest. For SOI, the statistical relationship begins to reverse in southern California, with a

tendency for above normal streamflow during El Nino, a relationship observed in seasonal precipitation that has been noted by Schonher and Nicholson (1989). This is an example where the statistics are weak even though there have been individual El Nino cases such as in 1982/83 and 1940/41 when the stormy North Pacific El Nino effect spread throughout much of the West. Statistically, the circulation pattern that is best correlated with anomalous precipitation and streamflow in California has negative geopotential or SLP anomalies just offshore, centered at about (40°N, 130°W) (Klein and Bloom 1987; Cayan and Peterson 1989). The winter 700-mb height teleconnection pattern centered at this origin (Namias 1981) illustrates this connection. In comparison to the Aleutian low teleconnection in the central North Pacific, the California pattern is more

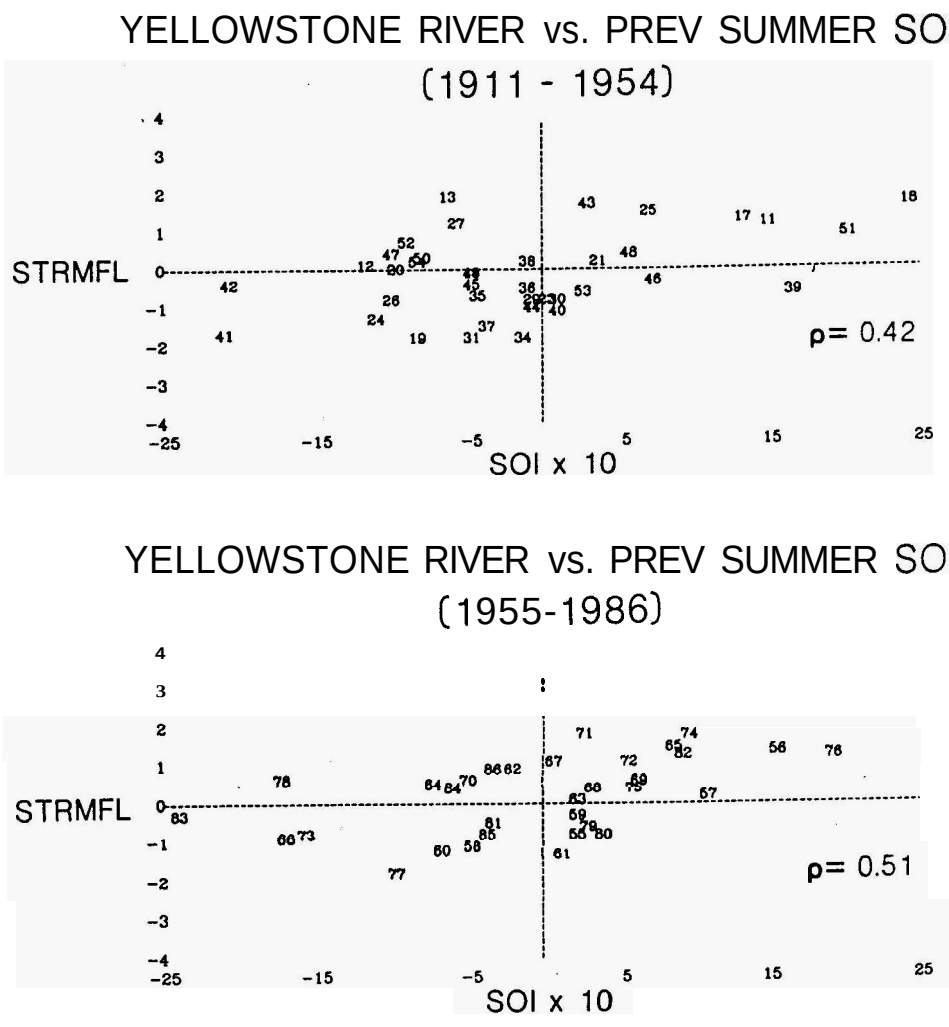

Fig. 3.4 *(a)* Summer SOI leading standardized December–August streamflow for Yellowstone River. Record is divided into two sections, 1911–1954 (top) and 1955–1986 (bottom). Year of each data point is labeled on plots as year-1900. Correlation (rho) is indicated for each period. (b) Same as (*a*) but for Salt River, whose two sections are 1914–1954 (top) and 1955–1985 (bottom).

regionally confined, and not well related to anomalies in the Aleutian Low region. For coastal British Columbia, a similar offshore regional atmospheric circulation pattern is associated with streamflow anomalies (Cayan and Peterson 1989). These more regional circulation connections explain the lack of a statistical connection between streamflow in these areas and strong or weak atmospheric circulation in the central North Pacific. Stated differently, California and British Columbia are close to the node of the atmospheric long-wave pattern that emanates from the central North Pacific, and small variations in the position of the remote circulation anomaly center can yield both positive and negative precipitation variations.

There is an important distinction between the results with streamflow and the results of Ropelewski and Halpert (1986). These authors found some evidence that the El Niño phase of ENSO was associated with lighter than average

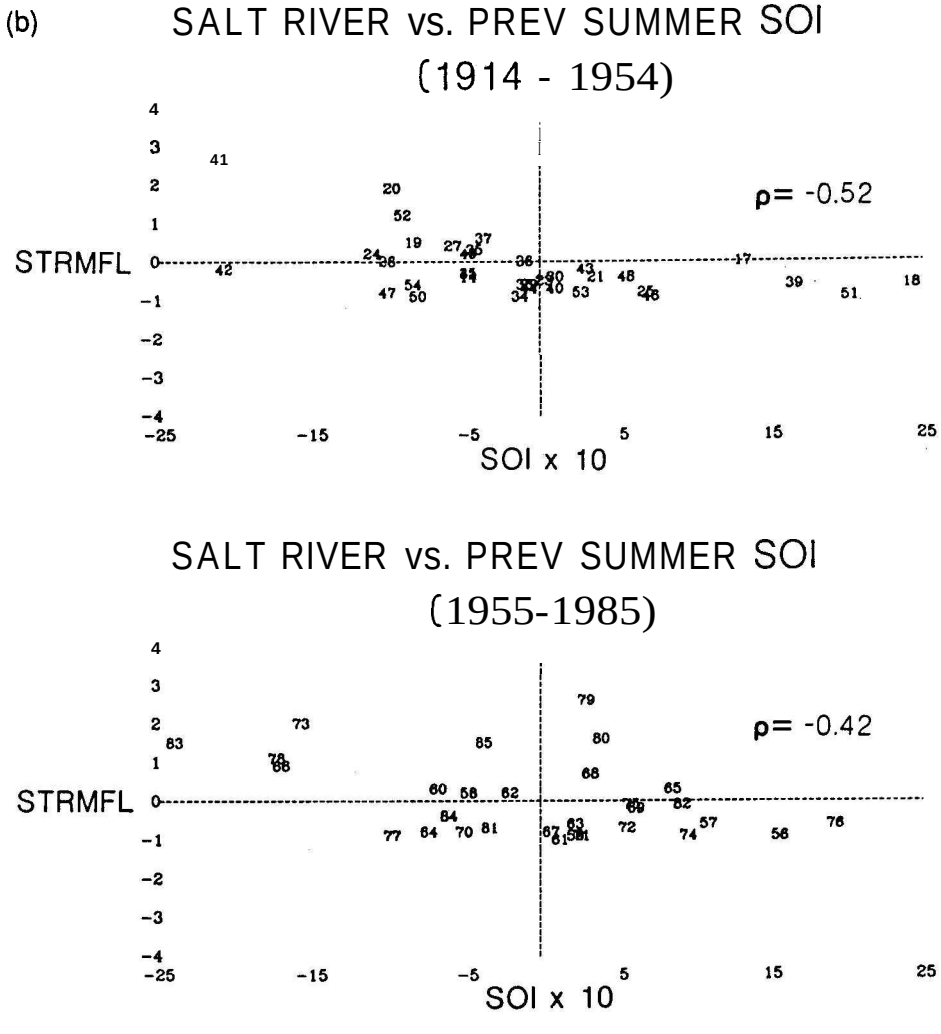

Fig. 3.4 *(b)*

precipitation in the Pacific Northwest, but this tendency was not strong enough for them to consider it to be reliable. The weakness in this relationship appears to arise, in part, from variations in the timing of the dry conditions between fall and spring of the mature El Niño period. However, the snow courses considered and the streamflow in basins with higher elevations are not as sensitive to these timing changes as is the precipitation, since SWC is cumulative and snowmelt constitutes a significant portion of the streamflow. Heavy Southwest runoff appears to result from active southerly-displaced middle-latitude storms that tap subtropical Pacific moisture, which is often transported by the subtropical jet stream. Heightened activity occurs over several months from fall through spring, as discussed by Douglas and Englehart (1981), Ropelewski and Halpert (1986), and Andrade and Sellers (1988), and as indicated by the frequency of daily precipitation discussed below. Increased precipitation in the Southwest occurs during late fall through spring in the El Nino phase of the Southern Oscillation, which would contribute to above-normal SWC in the higher elevations and also enhanced streamflow. To investigate the temporal consistency of the relationship between SOI and streamflow, the relationship was examined for two halves of the data period (before and after 1955). Figure 3.4 shows a pair of scatter plots of summer SOI vs. December–August streamflow at Yellowstone River and Salt River. While the correlations between SOI and streamflow in the Northwest and in the Southwest are not strong, these plots are fairly consistent from the early to the later period. For the earlier and later halves of the data, the Yellowstone and Salt River correlations are 0.42, 0.51 and −0.52, −0.42, respectively.

Daily precipitation

For more detail of the ENSO effects exposed by the seasonal relationships, the behavior of daily precipitation during different phases of the ENSO cycle was investigated. Two individual watersheds were studied, representing the core regions of the positive and negative SOI-SWC correlation patterns discussed above. These were the Yellowstone River, near the Corwin Springs, Montana gauge in the heart of the El Nino winter dry region in the Northwest, and the Salt River near the Roosevelt, Arizona gauge in the El Niiio winter wet region in the Southwest. The daily precipitation is broken into five successively heavier classes: all days with equal or greater than 1, 5, 10, 20, and 30 mm. In this categorization, the higher precipitation categories overlap each of those that are lower; e.g., all the days with 5 mm and greater precipitation are included in the 1 mm and greater category, and so on. Diaz (1991) has examined changes in different categories of United States regional precipitation according to longer period wet and dry regimes. The present analysis takes a similar approach, but here we explicitly considered the effect of ENSO. The El Nino and La Niña years employed in this analysis are shown in Table 3.1. The three 'seasons' employed were fall (August, September, and October, abbreviated ASO), early winter (November, December, and January, abbreviated NDJ), and late winter/early

spring (February, March, and April, abbreviated FMA). These seasons are centered on the mature northern winter phase of the warm or cold event, or 'year 1' of Rasmusson and Carpenter (1982) and Kiladis and Diaz (1989). For example, for the El Nino with mature phase in winter of 1973, NDJ is November and December 1972 and January 1973; FMA is February, March, and April 1973. Two fall seasons were included, designated ASO(0) and ASO(1), which in the example would be August, September, October 1972, and August, September, October 1973, respectively. To avoid mid-summer behavior within the fall aggregate, the ASO definition was from 15 August through 31 October.

First, consider Yellowstone River in the positive SWC and streamflow vs. SOI correlation region of the northwestern United States. The number of days with measurable precipitation, the amount of precipitation per day on days with precipitation, and the frequency of different categories of precipitation during El Niño, La Niña, and 'other' years, stratified by season is presented in Table 3.4. For Yellowstone River, the greatest difference between El Nino, La Nina, and 'other' year precipitation frequency is for the NDJ period. Considering daily precipitation of all amounts (greater than 1 mm), the mean precipitation over all precipitation days for the 18 El Niño years, the 12 La Nina years, and the 36 'other' years was 3.5, 4.4, and 3.7 mm d^{-1}, respectively. The frequency of NDJ daily precipitation of all amounts was lowest for El Niño (42.0%), greatest for La Niña (52.2%), and intermediate for 'other years' (47.5%). A higher frequency of precipitation during La Nina and lower frequency during El Nino prevailed for each successive category, especially for precipitation categories greater than 10 mm. The most impressive differences in precipitation frequency occurred in the higher daily precipitation categories. For example, days with 10 mm and greater precipitation were three times as likely to occur during La Nina (5.8%) as they did during El Niño (1.8%), and nearly twice as likely during 'other years' (3.1%). Although there are few days upon which to base a comparison, the only two days in the 64-yr period with greater than 30 mm were in La Nina years.

The other seasons at Yellowstone River showed less disparity in their El Nino, La Niña, and 'other year' frequencies, although FMA and ASO(0) exhibited a higher frequency of precipitation during La Nina than during El Nino. 'Other years' had nearly the same or a slightly higher frequency of most categories of precipitation as the La Nina years for these seasons, however.

To test the statistical significance of these differences, the following Monte Carlo exercise was performed. Sets of years equal in number to the available period of record were randomly chosen from the record. This random mix of years, whose numbers were the same as the years in the El Nino, La Niña, and 'other' year categories, was repeated 100 times, and each time the precipitation frequency statistics were computed. To preserve the annual distribution of precipitation, the daily precipitation within each year was retained unscrambled. The likelihood of achieving the observed El Niño, La Niña, and 'other' year statistics was judged by comparing the observed frequency or amount of daily precipitation (broken into the various precipitation amount bins) with that from

Table 3.4 *Daily precipitation statistics Yellowstone River region (1924–1988)*

	ASO (0)			NDJ			FMA			ASO (+1)		
	E[a]	L[a]	O[a]	E	L	O	E	L	O	E	L	O
No. days	1460	843	2737	1653	1063	3213	1683	1046	3070	1437	913	2620
No. days w/Ppt	406	259	835	695	555	1525	645	456	1343	395	261	844
Mean daily Ppt[b]	4.0	4.8	4.2	3.5	4.4	3.7	3.5	3.6	3.7	4.4	4.1	4.2
Ppt ⩾ 1 mm[c]	27.81	30.72	30.51	42.04	52.21	47.46	38.32	43.59	43.75	27.49	28.59	31.38
⩾ 5 mm	8.22	10.91	9.68	11.74	17.12	12.82	9.39	11.66	11.56	9.46	9.42	9.48
⩾ 10 mm	2.67	4.15	3.22	1.81	5.83	3.14	2.14	2.77	3.29	3.55	2.63	3.23
⩾ 20 mm	0.21	0.71	0.29	0.12	0.66	0.19	0.18	0.29	0.23	0.28	0.11	0.45
⩾ 30 mm	0.00	0.12	0.04	0.00	0.19	0.00	0.06	0.00	0.00	0.07	0.00	0.04

[a]E, L, and O designate seasons occuring within El Niño, La Niña, or "other" years.

[b]Mean daily precipitation for days with measurable precipitation; days with no precipitation are not included.

[c]Entries under each precipitation (ppt) category are the percentage of all days during period with ppt amount equal or exceeding that category's threshhold. Lower threshhold categories include days entering higher threshhold categories (e.g., days with 5 mm and greater are included in the 1 mm and greater category).

the 100 randomly generated sets of the three categories of years. The rank of the frequency or amount of the observed precipitation defined its percentile placement within the sorted (lowest to highest) stack of the frequency or amount statistics from the randomly generated sets.

First considering Yellowstone River, to assess the significance of these El Niño vs. La Niña differences, observed precipitation frequency and amounts for each category were compared with those from the stack of 100 Monte Carlo runs. At Yellowstone River, the NDJ results had interesting differences in comparison with the Monte Carlo series. For all precipitation days greater than 1 mm, the difference in precipitation frequency was not extremely unusual, but the difference in the amount of precipitation was quite significant. The frequency of El Niño precipitation days was ranked 14, and the La Nina precipitation frequency ranked 69. That is, 86 of the shuffled NDJ series had a frequency of precipitation higher than that of El Niño, and 31 of them had a frequency greater than that of La Nina. (Remember the rank is the percentile order from 1–100 of the sorted [lowest to highest] Monte Carlo precipitation series.) The amount of precipitation on all NDJ El Nino precipitation days was ranked 2, and on all La Niña precipitation days ranked 99. That is, 98 of the shuffled winter series had precipitation amounts greater than that of El Nino, and only 1 had an amount greater than that of La Nina. Thus a rainy day during La Nina had significantly heavier precipitation than a rainy day during El Niño. This difference in amounts is related to the frequency of larger precipitation amounts during El Nino versus La Nina years. While the larger amounts contribute a much smaller sample, the differences in the higher amount frequencies appear to be considerably more unusual than those of the all-precipitation-amounts frequencies. For days with 10 mm or more precipitation, the observed El Niño frequency ranked 0 (lowest), and the La Nina frequency ranked 100th (highest), among the 100 Monte Carlo series; that is, none of the Monte Carlo year series had frequencies as extreme. Results for the other seasons at Yellowstone River were not as significant (Table 3.4); i.e. the frequency and amount of daily precipitation during El Niño and La Nina differed little more than one would expect by chance.

Second, consider the Salt River, in the heart of the negative SWC and streamflow vs. SOI correlation region of the southwestern United States (Table 3.5). For Salt River, the greatest difference between El Niño, La Nina, and 'other year' precipitation frequencies was during FMA, and to a lesser extent, during NDJ. For FMA, considering all daily events, the mean precipitation showed opposite differences as those for Yellowstone River. Over all FMA precipitation days for the 24 El Nino years, the 16 La Niña years, and the 47 'other' years, the mean precipitation was 4.8, 4.3, and 4.6 mm d^{-1}, respectively. Correspondingly, the frequency of daily precipitation of any amount was highest during El Niño (24.8%), lowest during La Niña (14.9%), and intermediate during other years (21.2%). As they were at Yellowstone River, the differences were accentuated for higher precipitation amounts. At Salt River, days in FMA with precipitation equal or greater than 10 mm were about twice as likely during El

Table 3.5 *Daily precipitation statistics Salt River region (1901–1988)*

	ASO (0)			NDJ			FMA			ASO (+1)		
	E[a]	L[a]	O[a]	E	L	O	E	L	O	E	L	O
No. days	1925	1232	3619	2219	1523	4288	2250	1440	4230	1925	1232	3619
No. days w/Ppt	560	329	1049	495	273	914	557	214	895	537	381	1020
Mean daily Ppt (mm)[b]	4.3	4.4	4.2	5.9	5.2	5.5	4.8	4.3	4.6	4.2	4.3	4.3
Ppt ≥ 1 mm[c]	29.09	26.70	28.99	22.13	17.93	21.32	24.76	14.86	21.16	27.90	30.93	28.18
≥ 5 mm	9.09	7.79	8.93	9.37	7.35	8.26	8.36	4.58	7.26	8.10	9.74	8.79
≥ 10 mm	2.81	3.33	2.68	4.24	2.69	3.73	3.42	1.74	2.79	2.91	2.92	2.76
≥ 20 mm	0.42	0.65	0.47	1.17	0.66	0.77	0.58	0.28	0.40	0.57	0.49	0.44
≥ 30 mm	0.10	0.16	0.17	0.23	0.13	0.19	0.22	0.07	0.09	0.10	0.16	0.17

[a]E, L, and O designate seasons occuring within El Niño, La Niña, or 'other' years.

[b]Mean daily precipitation for days with measurable precipitation; days with no precipitation are not included.

[c]Entries under each precipitation (ppt) category are the percentage of all days during period with ppt amount equal or exceeding that category's threshhold. Lower threshhold categories include days entering higher threshhold categories (e.g., days with 5 mm and greater are included in the 1 mm and greater category).

Niño (3.4%) than during La Niña (1.7%) and about 1.2 times as likely during El Niño than during other year FMAs (2.8%). Days with 30 mm and greater precipitation occurred about 3 times more frequently during El Niño than during La Niña and more than two times more frequently than during 'other years.'

The Salt River NDJ differences were not as distinct as those for FMA. This was largely due to the frequency of occurrence of lighter precipitation days, which was more similar across the El Niño, La Niña, and 'other year' types. Days with less than 10 mm still occurred most frequently during El Niño (18.1 %), least during La Niña (15.2%), and intermediately during other NDJs (17.6%), but these differences were fairly bland. (The frequency of days with less than 10 mm is obtained by subtracting the frequency of greater than or equal 10 mm days from the frequency of greater than or equal 1 mm days.) For the larger daily precipitation categories, the relative differences were greater. Daily precipitation for NDJ greater than 10 mm occurred 1.6 times as often during El Niño (4.2%) as during La Nina (2.7%) and also more frequently during El Niño than during other years (3.7%).

To determine the significance of these Salt River precipitation frequency and amount differences among the three categories of years, they were each compared with the stack of 100 Monte Carlo precipitation frequency calculations. Compared to the Monte Carlo series, the Salt River FMA results were highly significant. Considering all precipitation days of any amount (greater than 1mm), the ***frequency*** of precipitation during El Nino was ranked 100, and the frequency during La Nina ranked 1. That is, none of the shuffled Salt River FMA series had a frequency of precipitation as high as that which occurred during El Nino years or as low as that which occurred during La Nina years. Differences in FMA daily precipitation ***amounts*** were not as remarkable, however. For FMA precipitation days of any amount (greater than 1 mm), the mean daily observed precipitation during El Niño ranked 78 and the mean daily observed precipitation during La Nina ranked 28 in the stack of 100 Monte Carlo sets. While drawn from a much smaller sample of days, the frequency of larger precipitation amounts during El Niño and La Nina was quite significant. For example, considering only days with precipitation of 10 mm or more, the observed El Nino frequency ranked 95th, and the La Niña frequency ranked 7th.

Results for NDJ at Salt River were not as significant, but were nonetheless consistent with those for FMA. For all precipitation days greater than 1 mm, the frequency of El Niño precipitation was ranked 70th, and the La Niña precipitation was ranked 20th. That is, of 100 Monte Carlo series, 30 NDJs had a higher precipitation frequency than the NDJ history for El Niiio, while 20 had a lower NDJ precipitation frequency than the NDJ history for La Niña. For all NDJ precipitation days greater than 1 mm, the mean amount observed on El Nino precipitation days was ranked 78 and the mean amount observed on La Niña precipitation days was ranked 28. Considering only days with 10 mm or greater precipitation, the El Niño frequency ranked 85th and the La Niña frequency ranked 4th.

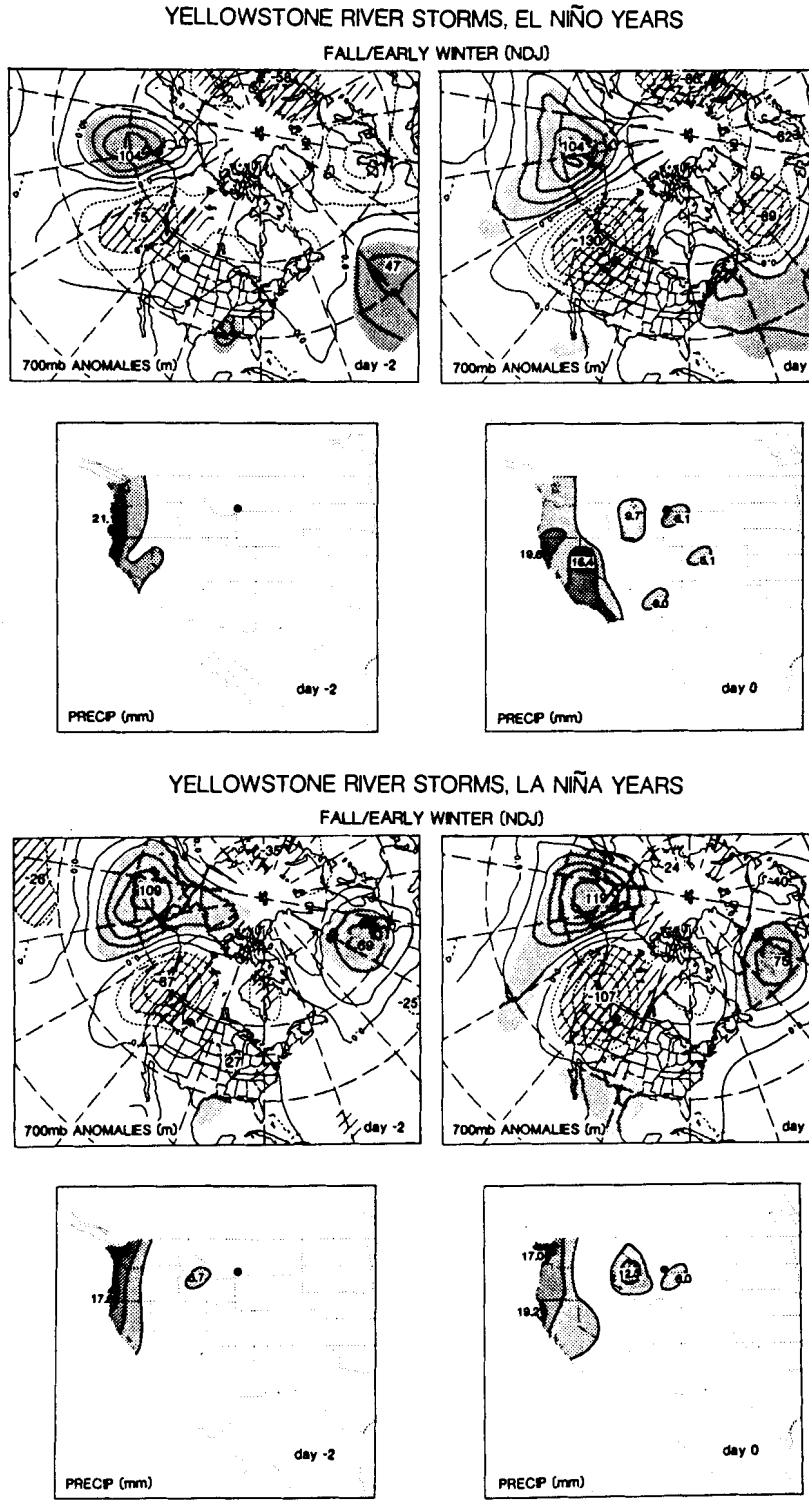

Fig. 3.5 A composite 700-mb height anomaly (m) and gridded precipitation anomaly (mm) for day −2 and day 0 of heavy (≥10 mm) daily precipitation events at Yellowstone River during November/December/January (NDJ). El Niño year cases are above and La Niña year cases below. 700-mb heights are from 12 00 GMT gridded

Daily atmospheric circulation

The Yellowstone River and Salt River daily precipitation show that the El Nino and La Niña phases of ENSO tend to produce opposite behavior of precipitation frequency and amounts. For further insight into the causes of daily precipitation associated with ENSO, we examined the atmospheric circulation and the spatial distribution of precipitation during heavy precipitation events of Yellowstone River and Salt River. The events considered were grouped by season (fall/early winter, or NDJ, and late winter/spring, or FMA) and by ENSO year type (El Niño or La Niña). The composites were based upon days with equal or greater than 10 mm of precipitation at the six stations of each basin. For groups with an ample number of heavy precipitation days, the threshold was raised to 15 mm of precipitation. These days were selected from the 1947–1988 period. The composite contained as few as 7 cases and as many as 24 cases. In an attempt to provide an independent set, consecutive days which happened to exceed the 10 mm threshold were eliminated by only including the first day of the episode. Both 700-mb height anomalies over the western part of the Northern Hemisphere and gridded precipitation over the western United States are mapped for these days. To provide an indication of the development of the precipitation event, these fields are shown for two days beforehand (day -2) as well as the day of the composite event. The statistical significance of the 700-mb height anomalies is indicated by a two-tailed t-test. Values exceeding the null hypothesis (no difference in pattern from the long-term mean) at the 95% level of confidence are shaded. Since by chance, it might be expected that a certain number (50 or less) of the 360 grid points comprising this field would contain a 700-mb anomaly composite exceeding the 95% confidence threshold, the composite anomalies were tested for field significance (Livezey and Chen 1983). Each of the maps in the following set of analyses contains more grid points with significant composite anomalies than would be expected by chance (95% of the time) using a Monte Carlo procedure. Moreover, these maps are meaningful because the anomalies form physically reasonable patterns associated with the regional precipitation considered.

As indicated by the 95% confidence level (relative to the null hypothesis) shaded regions on the 700-mb anomaly composites, the patterns involved in the precipitation events are quite distinct from a random sample. By inference from the shading pattern, the El Niño vs. La Nina maps are nearly indistinguishable for the NDJ sets but they are quite different for the FMA sets. As will be seen, this difference between NDJ and FMA occurs for both Yellowstone River and Salt River precipitation patterns.

Figure 3.5 shows the composite 700-mb height anomaly and precipitation distribution for fall/early winter at Yellowstone River during El Niño and La

Fig. 3.5 (*cont.*) analysis from days entering the composite. Regions of composite anomalies significant at the 95% confidence level are indicated by shading. Shading of precipitation indicates regions with equal or greater than 5, 10, and 15 mm.

Niña. The atmospheric circulation patterns for El Niño and La Nina are very similar in the North Pacific–western North America sector. Both have well defined patterns, with a strong positive anomalies to the west over the North Pacific and negative anomalies over the eastern North Pacific and western North America. The positive anomalies are centered in the Aleutian Island–Bering Sea region and the negative anomalies are centered in Washington State. This pattern induces a southwesterly flow into the central Rockies region that includes Yellowstone River. The precipitation maps indicate that the heavy precipitation associated with this pattern usually develops out of a system which first appears over coastal Washington, and propagates eastward into the Rockies. The precipitation is regional in scope, as evidenced by the several grid points having precipitation exceeding 5 mm (note that the precipitation on the grid point maps may appear spotty because some stations fall below the threshold chosen for the shading.) There is a systematic development over at least 2 d, as indicated by the day -2 composite 700-mb height anomalies: note the already strong positive anomaly center upstream in the Aleutian Islands. In fact, this development can be traced back at least 4 d beforehand (maps not shown). The greatest dissimilarity in the El Niño vs. La Niña patterns occurs downstream over the North Atlantic south of Greenland, where the El Nino circulation has a strong negative anomaly and the La Nina circulation has a positive anomaly.

The late winter spring circulation patterns for Yellowstone River (Fig. 3.6) offer much greater contrast. The El Niño pattern exhibits negative 700-mb height anomalies across the entire North Pacific basin north of 30°, culminating in a negative anomaly center just west of Washington State. Strong southwesterly wind anomalies again occur over the central Rockies. In the Pacific sector, the La Niña pattern has an anomaly structure which is somewhat more spatially confined than that of El Niño. Negative anomalies of this pattern are located north of the Bering Sea and in the Gulf of Alaska, and extend over much of the southern Canada and the northern coterminous United States. Over the North Pacific, the lack of distinct anomalies reflects a lack of consistency in the pattern there; evidently there are several upstream circulation patterns contributing to La Niña precipitation. In common with all the other composites this late winter/spring pattern has negative 700-mb height anomalies over the West and anomalous southwesterly flow into the central Rockies. Here, the negative anomalies are shifted farther east than for the other cases, however, with a center over Idaho. Downstream, another interesting feature of this pattern is the couplet of strong negative anomalies south of Greenland and positive anomalies over Scandinavia. Inspection of composite maps subsequent to this event (maps not shown) indicate that this downstream anomaly continues to grow, with centers exceeding 200 m. (Apparently in some cases, rain in Montana is a good predictor of European weather conditions, although this suggestion should be examined using a larger sample.)

Even though the Salt River basin is more than 10° latitude south of the Yellowstone region, the Salt River 700-mb composite patterns during heavy

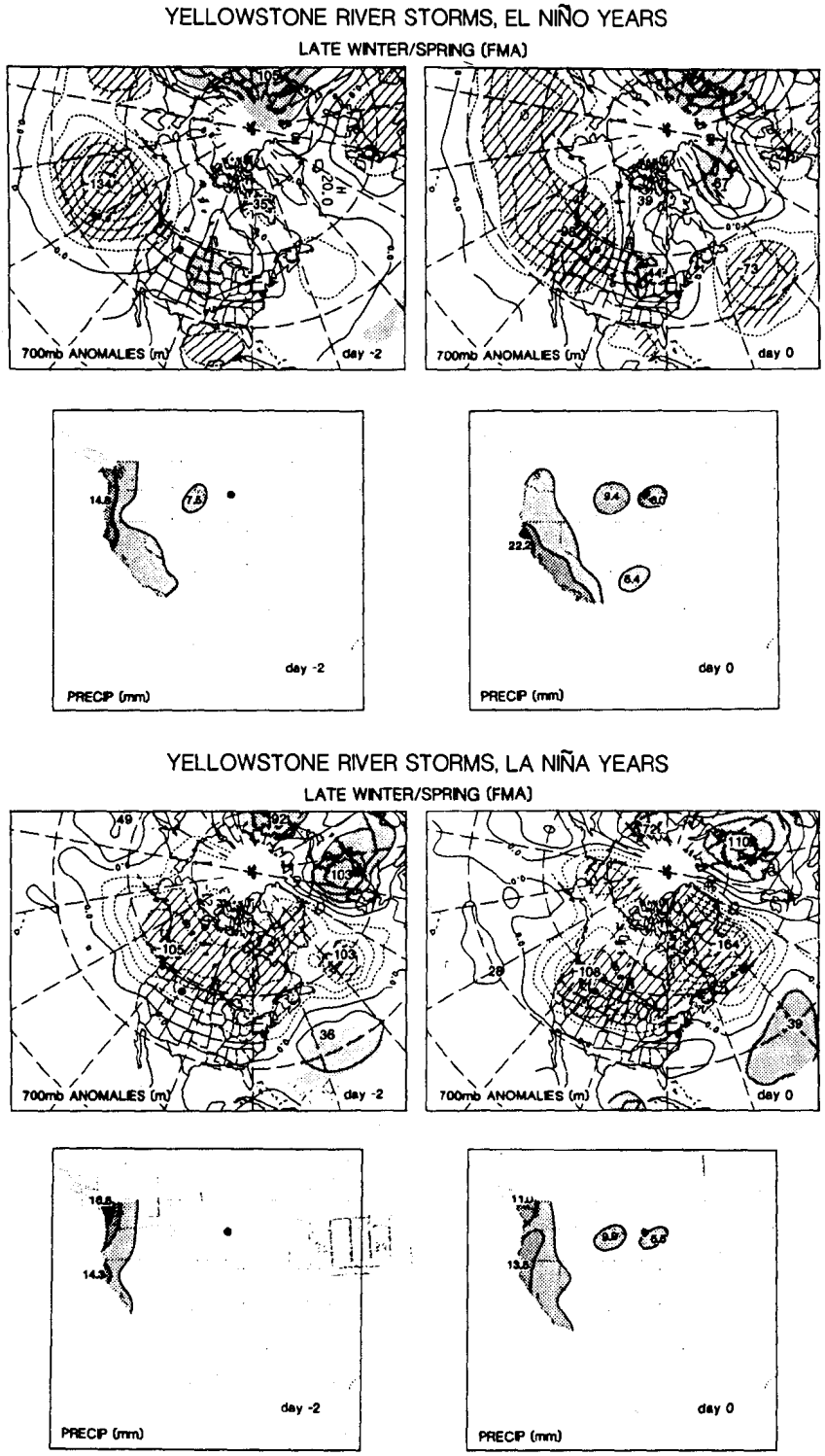

Fig. 3.6 Same as Figure 3.5, but for FMAs of El Niño years, Yellowstone River.

precipitation days have a resemblance to those for Yellowstone. For Salt River, the El Niño and La Niña heavy precipitation patterns are much alike in NDJ (Fig. 3.7) but quite different in late winter/spring. The El Niño and La Niña fall/early winter patterns are both examples of the development of sharp troughs along the West Coast, probably including a number of 'cut-off lows' (see discussion on flood events below). In both composites, the event is preceded on day −2 by the development of large positive anomalies (a high pressure ridge) upstream in the Gulf of Alaska, as well as a significant negative anomaly region (a trough) stationed just off the northern California coast. By the day of the event, the negative anomaly has strengthened and moved southeastward to a position near southern California, and a strong positive anomaly just downstream over the eastern United States, centered over the Ohio Valley. Regionally, in the transition from day −2 to day 0, strong southwesterly flow develops over southern Arizona, and the precipitation spreads from coastal Washington, Oregon, and northern California to southern California and Arizona.

The late winter spring (FMA) patterns at Salt River are quite different between El Niño and La Niña (Fig. 3.8). The La Niña pattern has local negative 700-mb height anomalies and a strong positive anomaly in the eastern Gulf of Alaska. This pattern is somewhat similar to the 'sharp trough' pattern observed in NDJ, with a strong positive anomaly to the northwest and a negative anomaly (cutoff low) centered at low latitudes (about 30°S, just offshore of Baja California, Mexico). This positive/negative anomaly couplet develops out of a strong negative anomaly far upstream to the south of Kamchatka on day −2. The gridded precipitation shows a drastic change from day −2 to day 0 of the La Niña event, with significant precipitation in western Washington on day −2 and then an isolated region of heavy precipitation in Arizona on day 0.

In contrast to the La Nina pattern, the El Niño late winter/spring pattern is a North Pacific basin wide negative anomaly which extends into the Southwest. This pattern represents an expanded circumpolar vortex, with strengthened westerly winds centered about 30°N, and positive 700-mb height anomalies far to the north over Alaska, central Canada, and south of Greenland in the North Atlantic. The movement of this system onshore from day −2 to day 0 is apparent from the two 700-mb anomaly patterns as well as from the precipitation maps, which indicate heavy precipitation in California on day −2 spreading to Arizona and southern New Mexico by day 0.

The limited sample size in these composites may allow the resulting anomaly field to be heavily biased by an unusual pattern during one particular year. One reviewer cautioned that the impressive FMA anomaly patterns for the Yellowstone River and Salt River El Niño composites might have been largely produced by the strong El Niño of winter 1983. For Yellowstone River, only one of the 12 cases included in the composite was from 1983, so that this pattern is not dominated by the winter of 1983. The Salt River FMA composite consisted of 18 individual storm cases, of which 4 storms were from 1983, so that may have had a significant impact. However, we tested this by removing these four cases

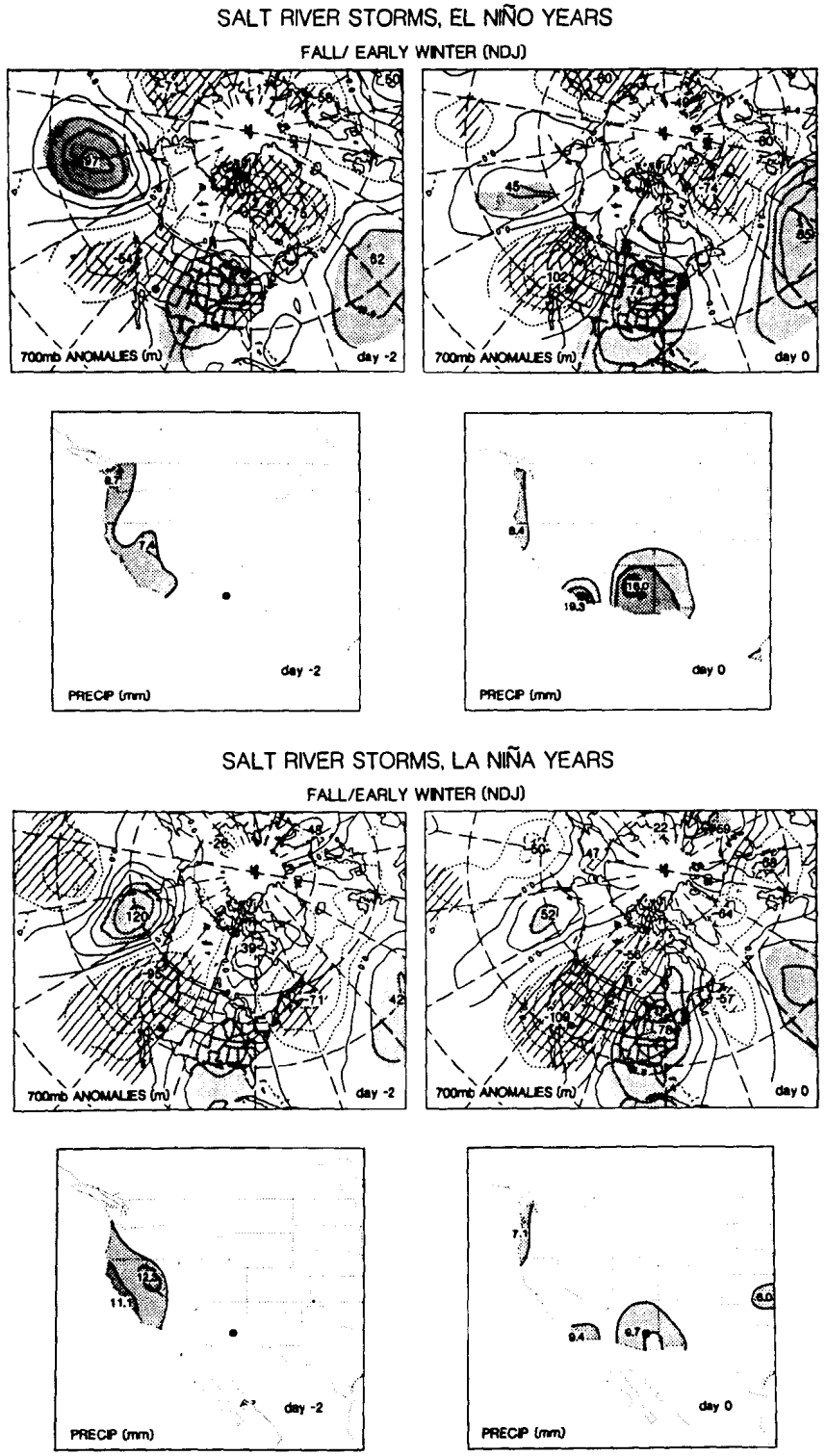

Fig. 3.7 Same as Figure 3.5, but for NDJs of El Niño years, Salt River.

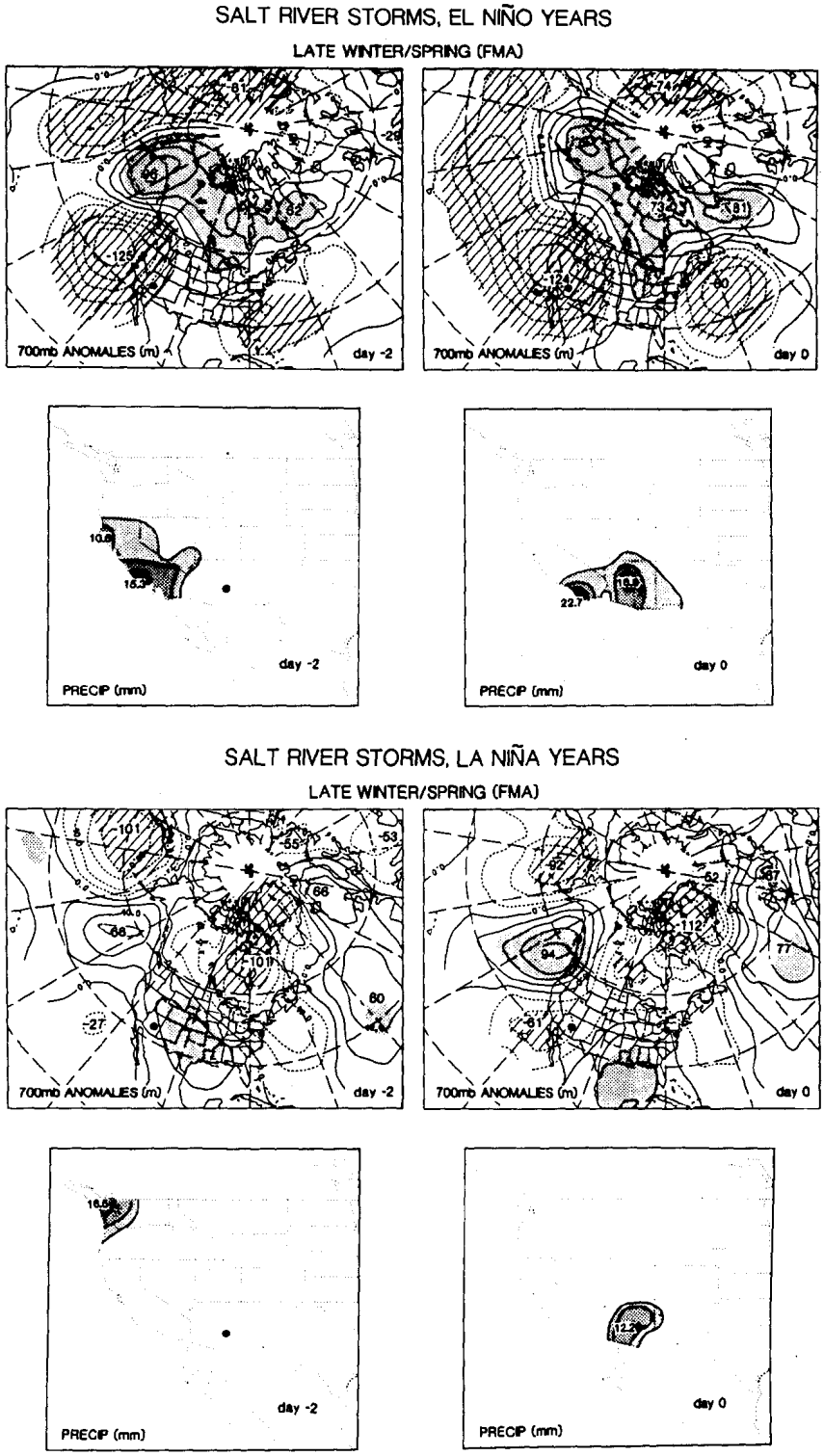

Fig. 3.8 Same as Figure 3.5, but for FMAs of El Niño years, Salt River.

and re-computing the composite. The resultant map, while not quite as strong as the original, had the same pattern, so it appears that the FMA vs. NDJ composite differences are robust.

El Nino and flood frequency

In the southwestern United States, the statistically significant negative relations between SOI and precipitation and SOI and streamflow suggest that El Nino and large floods should be related. During El Nino, atmospheric circulation is unusual and anomalously warm water in the eastern Pacific Ocean provides a source for large amounts of precipitable moisture. Therefore, the hydroclimatology of storms that cause floods should be different during El Nino conditions. For example, the hydrograph and associated precipitation of exceptionally large floods on the Salt River near Roosevelt, Arizona, during the strong El Nino of

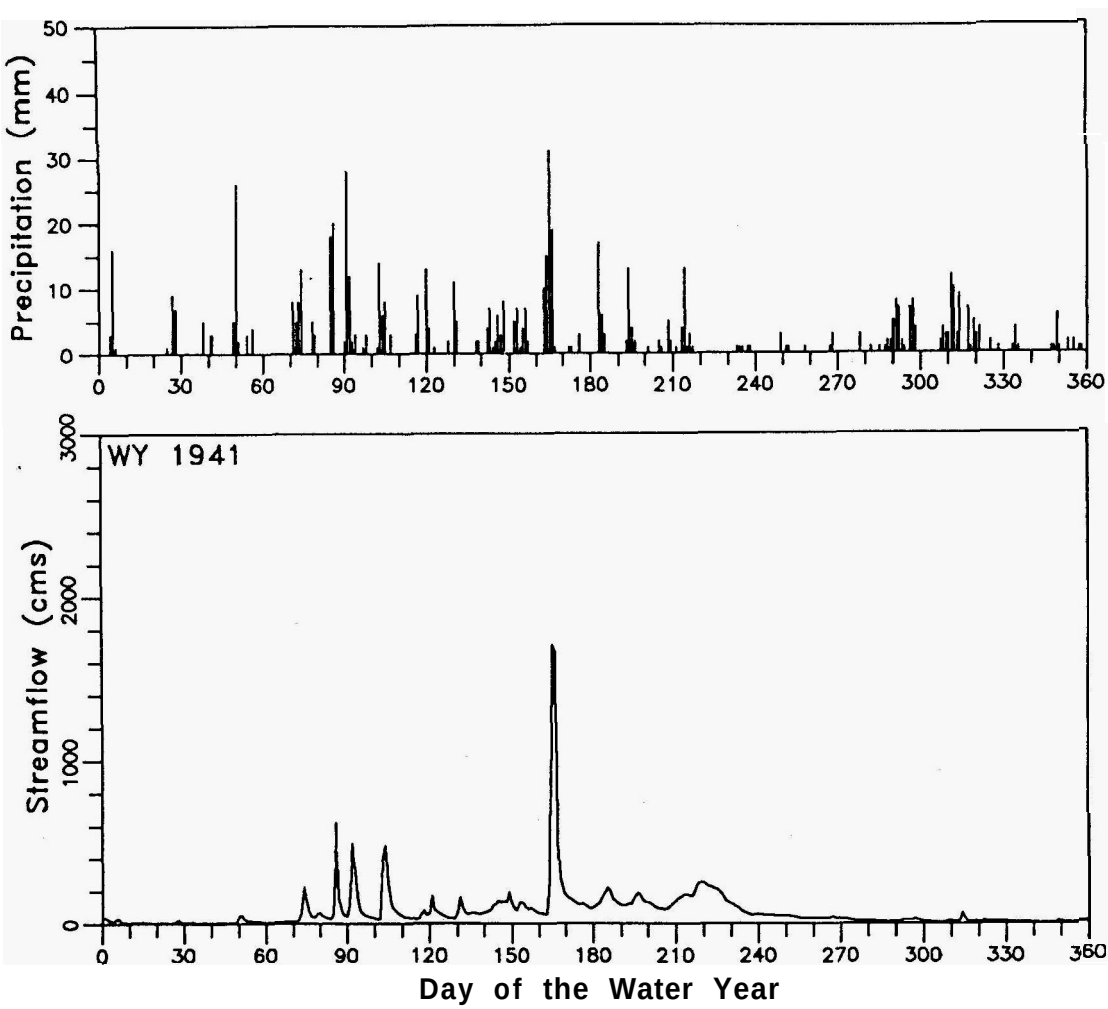

Fig. 3.9 Daily streamflow at Salt River ($m^3 s^{-1}$) and daily precipitation (mm) at Roosevelt, Arizona for water year (WY, October–September) 1941.

1941 is shown in Figure 3.9. Most of the largest floods on large rivers in Arizona have occurred during or within 6 mo following cessation of El Niño conditions (Table 3.6). Although most of the years in which large floods occurred have been rated at strong or very strong El Nino conditions (Quinn et al. 1987), others occurred under moderate or weak El Nino conditions (Table 3.6). Many of these rivers have headwaters in Colorado, Utah, or New Mexico, which underscores the large-scale nature of the anomalous circulation patterns, as illustrated in the previous section.

Flood frequency in Arizona is particularly sensitive to El Nino conditions because floods can occur in three distinct hydroclimatic seasons (Hirschboeck

Table 3.6 ***Recorded large floods on drainages larger than 3600 km^2 in Arizona during or within 6 months after El Nino conditions.***[a]

Year	Month	El Nino severity[b]	River gauging station	Peak discharge (m^3/s)	Rank of flood[c]
1862	Jan?	W/M?	Colorado River near Topock	11300	1
1862	Jan	W/M?	Virgin River at Littlefield	Unknown	1*
1868	Sep	M	Gila River at Kelvin	Unknown	2*
1884	Jul	S+	Colorado River near Grand Canyon	8500	1
1891	Feb	VS	Salt River near Roosevelt	Unknown	1*
1891	Feb	VS	Bill Williams River near Planet	5670	1
1891	Feb	VS	Verde River below Tangle Creek	4250	1
1905	Nov	W/M	San Francisco River at Clifton	1840	3
1905	Nov	W/M	Gila River at Kelvin	5380	1
1923	Sep	M	Little Colorado River at Grand Falls	3400	1
1926	Oct	VS	Paria River at Lees Ferry	456	1
1926	Sep	VS	San Pedro River at Charleston	2780	1
1941	Mar	S	Salt River near Roosevelt	3310	1
1966	Dec	M+	Virgin River at Littlefield	1000	1[d]
1972	Oct	S	Gila River at head of Safford Valley	2330	3
1972	Oct	S	San Francisco River at Clifton	1810	3
1977	Oct	M	Santa Cruz River at Tucson	651	2
1983	Oct	S	Gila River at head of Safford Valley	3740	1
1983	Oct	S	Santa Cruz River at Tucson	1490	1
1983	Oct	S	San Francisco at Clifton	2580	1

[a]Data from U.S. Geological Survey records.

[b]Strength of El Nino events is from Quinn et al. (1987), except for 1862 (Quinn, pers. comm., 1990). VS, very strong; S, strong; M, moderate; W/M, weak to moderate; +/– indicates an event between strength ratings.

[c]A rank of 1 is the largest flood of record.* indicates uncertainty because the flood was not part of the systematic gauging record but probably is of the rank listed.

[d]A larger flood in 1990 was caused by a dam failure.

1985, 1987). Floods commonly result from frontal storms in winter (November–March); Figure 3.7a and 3.8a give composite 700-mb height anomalies that are typically associated with this type of storm. During summer (July–August), advection of low-level moisture from the Gulf of Mexico and eastern North Pacific Ocean into the Southwest causes what is termed the Arizona 'monsoon,' which is characterized by local to mesoscale thunderstorms. However, summer thunderstorms do not cause the largest floods in Arizona (Table 3.6), except in small drainages (less than about 259 km^2). There have been large floods in fall (September–October), as moisture from dissipating tropical cyclones may be advected into the Southwest. This source has caused some of the largest floods in Arizona, particularly between 1972 and 1983 (Table 3.6). For the flood-frequency analysis discussed below, we have redefined the water year, which the U.S. Geological Survey conventionally defines as 1 October to 30 September, as 1 November to 31 October to be in accord with the hydroclimatological seasons.

Webb and Betancourt (1992) investigated the effects of low-frequency climatic variability on flood frequency of the Santa Cruz River in southern Arizona. Six of the ten largest floods at Tucson occurred during or within 6 mo following

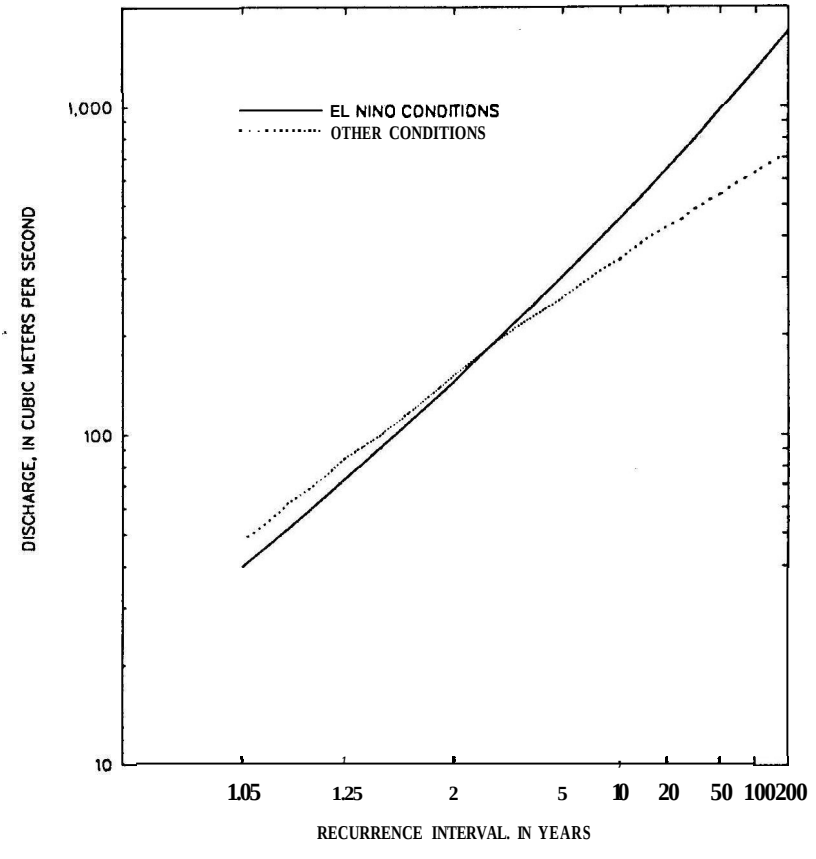

Fig. 3.10 Flood frequency for El Niño and other years for the Santa Cruz River at Tucson. Arizona. 1914–1986. (Modified from Webb and Betancourt 1992.)

cessation of El Niño conditions. Flood frequency was greater during El Nino conditions at recurrence intervals of greater than 10 yr (Fig. 3.10). The difference in flood frequency between El Nino and other conditions is caused primarily by a significant increase in variance of size of floods during El Niño conditions (Webb and Betancourt 1992); the mean annual flood was unchanged.

Flood frequency of the Salt River (Fig. 3.1) illustrates some of the problems associated with flood frequency in relation to El Niño and La Nina conditions. The two largest floods on the Salt River occurred during the El Niño years of 1891 and 1941 (Table 3.6). Although floods during El Niño years are nearly twice as large as floods during La Niña years at all recurrence intervals (Fig. 3.11), floods during other years are much larger than either at recurrence intervals greater than about 5 yr. Statistically, the differences among the different sets of years occurs in the skew coefficient, which is −0.44 for La Nina conditions, 0.20 for El Niño conditions, and 0.42 for other conditions. The differences in skew coefficients account for differences in the curvature of the flood-frequency relations (log-Pearson type 111 distribution); the more positive skew coefficients, such as calculated for El Niño and other years, cause an upward curvature in the

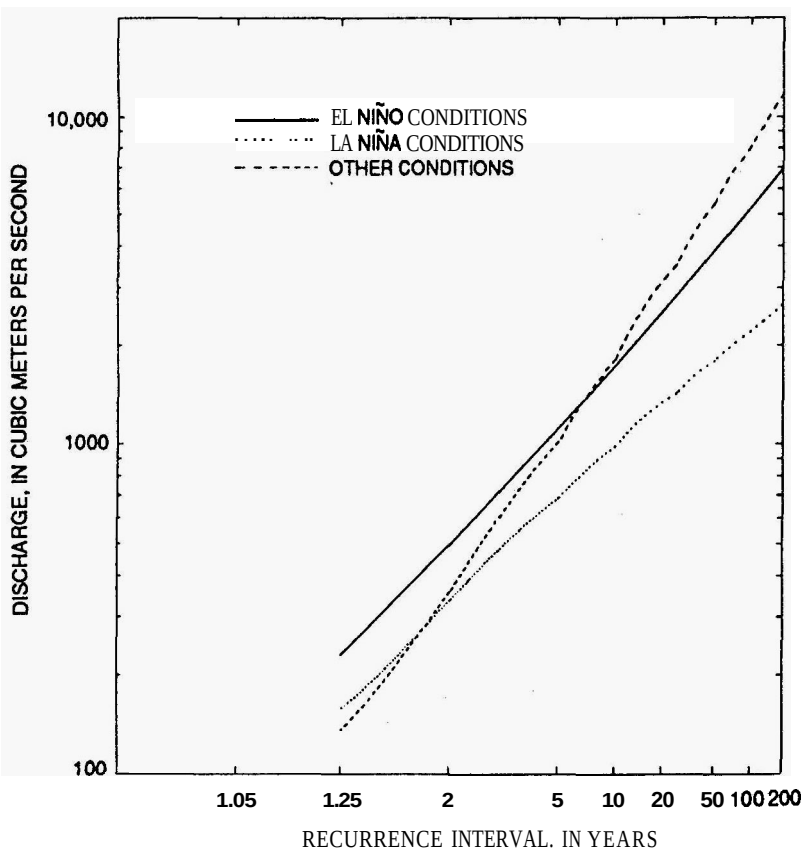

Fig. 3.11 Flood frequency for the Salt River near Roosevelt, Arizona, for El Nino, La Nina, and other years, 1925–1988.

relations (Fig. 3.11). Although it would appear from Figure 3.11 that El Nino has a minor effect on flood frequency of the Salt River, the results may be deceptive and influenced by lag effects of large floods which occurred in 1927, 1937, 1952, 1960, 1978, 1979, and 1980, none of which was an El Nino or La Nina year, but they were years with some months of negative SOI.

As this example shows, fundamental knowledge of hydroclimatic controls on flood frequency may not be gained from simple analysis of El Nino and La Nina conditions. Instead, the flood-generating mechanism, and the effect that El Nino may have on the mechanism, are of greater importance. Hirschboeck (1985, 1987) analysed flood-generating storm types in the Gila River basin of southern Arizona, and Webb and Betancourt (1992) combined many of Hirschboeck's storm types into the three types: frontal systems, monsoonal storms, and dissipating tropical cyclones. A fourth type of storm, cutoff low-pressure systems, occurs in fall to spring, but we had insufficient data to adequately account for floods caused by this type of storm. Nonetheless, cutoff low-pressure systems are considered here because of their influence as a steering mechanism for dissipating tropical cyclones in fall (Smith 1986). Analysis of the influence of El Nino on these storm types would result in a more direct examination of the causal mechanism of floods in the southwestern United States.

Storm types and floods affected by El Nino

In general, several climatic anomalies occur during El Nino conditions that affect storm types for the southwestern United States. As discussed earlier in this chapter, winter storms increase in severity and the amount of winter precipitation is increased during years with El Nino conditions. Not surprisingly, this leads to increased frequency of winter floods in some El Nino years, particularly on rivers in Arizona with extensive drainage areas at elevations greater than 2000 m. However, the effects of ENSO on other types of storms that may cause floods are more subtle and involve changes in sea-surface temperatures and atmospheric circulation.

During El Nino conditions, the anomalously warm pool of water in the eastern equatorial Pacific Ocean provides a source of precipitable moisture for advection into the extratropical latitudes. Also, the strength of the westerlies tends to increase, providing a steering mechanism for disturbances to move into the southwestern United States. Carleton et al. (1990) discuss in detail some of the atmospheric circulation mechanisms associated with variability of summer monsoon rainfall in the southwest United States and their relationship to ENSO phases,

The relation between El Niño conditions and tropical cyclones in the eastern North Pacific Ocean provides an example of the complex and interrelated changes associated with ENSO. The greatest incidence of tropical cyclones affecting Arizona occurs during or within 6 mo of cessation of El Niño conditions (Smith 1986; Webb and Betancourt 1992; Hereford and Webb in press). Most

tropical cyclones in the eastern North Pacific move in a westerly or northwesterly direction; ones that affect the continental United States must have sufficient longevity and concurrently favorable steering winds to recurve towards the northeast.

Generation of tropical cyclones in the eastern North Pacific Ocean is slightly suppressed during El Nino conditions and to a lesser extent during La Nina conditions (Table 3.7). Also, the number of days with hurricane conditions is also lower during El Nino and La Nina conditions (Table 3.7). These results are similar to previous findings for tropical cyclones in the Australian region (Nicholls 1985) and Atlantic Ocean hurricanes for El Nino conditions (Gray 1984). Reasons for the suppression of tropical cyclones in the eastern North Pacific may be increased vertical shearing in the atmosphere caused by increased upper-level westerlies and the southward shift of the ITCZ in those years.

As in the Atlantic Ocean, the number of tropical cyclones in the eastern North Pacific Ocean is not much below average for El Nino years between 1965 and 1990. Although the lowest annual numbers of tropical cyclones occurred in the El Nino years of 1969 and 1977, the second and third largest annual number of tropical cyclones occurred during and just after El Nino conditions in 1982/83 (Fig. 3.12). The above-average number of tropical cyclones between 1982 and 1987 (Fig. 3.12), and consequent increase in hurricane days, reduces the statistical certainty of decreased tropical cyclone activity during El Nino conditions by increasing the interannual variability.

The latitude and longitude of the origin point for tropical cyclones is an important factor in whether the storm may recurve towards the northeast and affect the continental United States. Storms that form too far south and/or west of the Pacific coast of Mexico or other Central American countries must travel farther to reach a position where they could affect the continental United States and are likely to be steered away from the mainland. During July–September of El Nino years, the average point of origin of tropical cyclones tends to be slightly west

Table 3.7 *Numbers of tropical cyclones and duration of hurricanes in the eastern North Pacific Ocean, 1965–1988, for El Nino, La Nina, and 'other' years*

	Number of years	Mean	Standard deviation
Number of tropical storms and hurricanes per year			
El Niño years	9	13.8	4.4
La Nina years	4	14.8	2.8
'Other' years	11	16.8	3.1
Hurricane days per year			
El Niño years	9	60	36
La Niña years	4	51	19
'Other' years	11	72	26

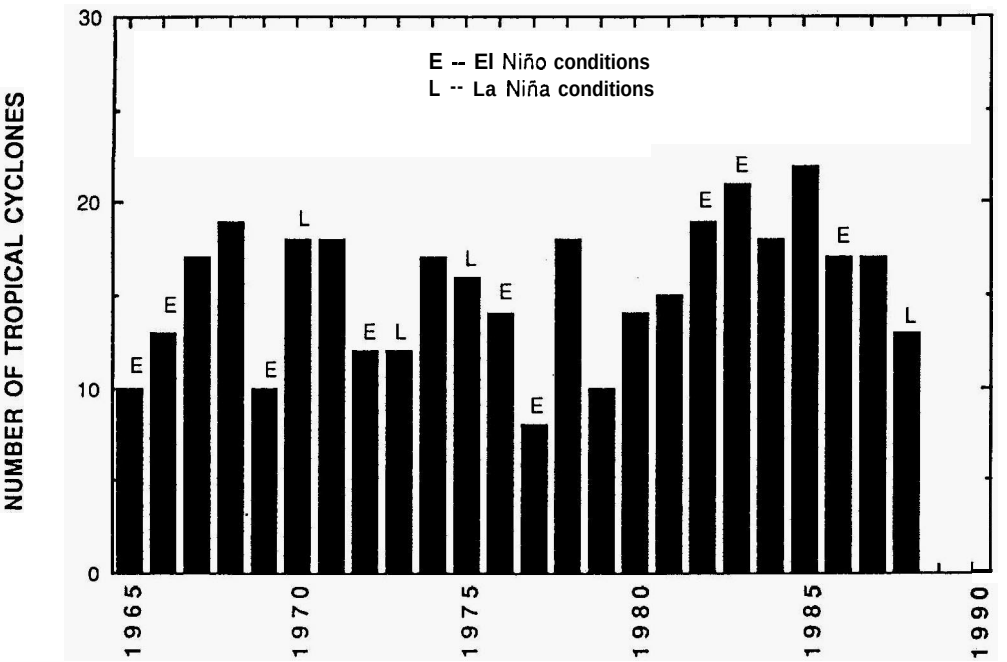

Fig. 3.12 Tropical cyclone occurrence in the eastern North Pacific Ocean, 1965–1988.

or southwest of the point of origin of tropical cyclones in other years (Table 3.8). Again, interannual variability precludes a conclusion of statistically significant changes, but the origin point appears to be shifting towards the pool of warmer water that tends to form off the west coast of Mexico during El Nino conditions. A shifting of the point of origin for tropical cyclones, albeit weak, has also been reported for the South Pacific (Revell and Goulter 1986).

During average El Niño years, fewer tropical cyclones are generated at points farther from the continental United States, and hurricanes that develop from these cyclones have a shorter duration. However, these averages are contrary to the fact that more tropical cyclones dissipate over the southwestern United Stated during or within 6 mo of cessation of El Niño conditions. El Nino-induced changes in the steering mechanism of most recurving tropical cyclones may explain why more tropical cyclones tend to recurve in years in which fewer tropical cyclones are generated.

Cutoff low-pressure systems interact with many tropical cyclones to cause recurvature and advect low-level moisture over the continent (Smith 1986). These upper-atmospheric cyclones often form during the transition from meridional flow to zonal flow and can be defined by examination of 500-mb daily-weather maps (Webb and Betancourt 1992). As Table 3.9 shows, the average number of cutoff low-pressure systems that occurred during El Niño and other years are 4.07 and 3.50, respectively, for fall months. Although large interannual variability precludes statistical significance (Table 3.9), it suggests that the probability

Table 3.8 ***Locations of origin and numbers of eastern North Pacific Ocean tropical cyclones during El Niño, La Niña and 'other' years, 1949–1989.***

Month		El Niño		La Niña		Other years	
		Latitude	Longitude	Latitude	Longitude	Latitude	Longitude
May	Number	5	5	0	0	5	5
	Mean	10.68	103.3	–	–	12.3	103.9
	Variance	4.44	46.8	–	–	4.0	76.0
June	Number	16	16	12	12	39	39
	Mean	12.98	100.99	12.8	100.4	13.1	103.2
	Variance	4.5	35.69	2.4	54.0	5.4	46.8
July	Number	27	27	19	19	65	65
	Mean	13.64	109.77	13.9	102.8	13.7	107.3
	Variance	8.57	126.64	5.2	48.8	6.9	68.9
August	Number	39	39	18	18	66	66
	Mean	13.63	112.69	13.9	108.6	14.1	112.5
	Variance	12.75	181.5	7.7	129.5	9.0	209.7
September	Number	54	54	22	22	60	60
	Mean	14.27	113.77	16.9	113.0	14.9	111.0
	Variance	8.57	352.3	22.5	413.9	10.2	377.7
October	Number	30	30	9	9	40	40
	Mean	13.47	106.96	12.6	105.0	14.1	108.8
	Variance	6.56	121.31	1.1	67.8	9.6	102.0

Table 3.9 *Number of cutoff low-pressure systems affecting the south western United States in fall and winter, 1945-1988, for El Nino, La Nina, and 'other' years.*

	Number of years	Fall Mean	(Sep-Oct) Standard deviation	Winter Mean	(Nov-Mar) Standard deviation
El Niño years	15	4.07	1.62	8.67	2.29
La Nina years	7	3.71	1.60	7.33	3.39
Other years	22	3.50	1.82	8.27	3.63

of occurrence a favorable steering mechanism may be slightly larger during El Nino conditions.

The example of the complex effect of El Niño conditions on tropical cyclones illustrates the complicated effects ENSO also has on southwest United States flood frequency. Under typical conditions, fewer cyclones may be generated with a shorter life expectancy, but the southward extension of the westerlies may increase the potential for recurvature. Moreover, the potential for a favorable steering mechanism, which typically is a cutoff low-pressure system, is also higher during average El Nino conditions. Nevertheless, this coincidence of favorable factors does not occur in all years with El Nino conditions; hence, flood frequency may be affected only in a small, as yet undefined subset of years with El Nino conditions.

Conclusions

Seasonal snow water content and streamflow are enhanced in the southwestern United States and diminished in the northwestern United States during the mature Northern Hemisphere winter phase of El Nino, and vice-versa during the corresponding phase of La Niña. There is also some evidence for increased streamflow along the Alaskan coast during El Nino. This is consistent with relationships between ENSO and precipitation, discussed by several previous authors. Areas such as California and British Columbia are not reliably connected to ENSO variations, but have been influenced by ENSO conditions in certain extreme cases. There is apparently some predictive value in the ENSO connection to streamflow in the southwestern and northwestern United States, albeit small in terms of variance accounted for. Correlations with the summer Southern Oscillation Index (SOI) leading the following December–August stream discharge have magnitudes of approximately 0.4, and are nearly as strong as those between winter SOI and December–August stream discharge. The reliability of these seasonal correlations appears to hold up from one period to the next; this was demonstrated by splitting the sample into halves and comparing the SOI vs. discharge correlations from the two for Yellowstone River in Montana, and Salt River in Arizona.

While the above correlations are weak, they are statistically significant at a fairly high level of confidence. Ropelewski and Halpert (1986) discounted the ENSO precipitation relationship in the Northwest and Southwest because these relationships were not strongly repeatable from one El Nino or La Nina event to the next. However, the distribution of daily precipitation, stratified seasonally, during El Nino years and during La Niña years appears to be quite distinct. This is demonstrated by randomly choosing sets of years corresponding to the number of years of El Nino and the number of years of La Nina from observed records in the heart of ENSO connections in the northwest and southwest United States. In this Monte Carlo exercise, the lowered frequency of precipitation observed during El Nino in November, December, and January (NDJ) and heightened frequency of precipitation observed during La Nina NDJs in the Yellowstone River, Montana region is unlikely to occur by chance. This difference between El Nino and La Nina is even more apparent in the frequency of heavy precipitation amounts (equal or greater than 10 $mm\,d^{-1}$) at Yellowstone River. In NDJ, the La Niña precipitation occurs about three times as often as during El Niño. Other years have a precipitation frequency intermediate between El Nino and La Niña. Differences are greater for high precipitation amounts than low precipitation amounts. Similar conclusions are drawn for Salt River, Arizona from analogous comparison between the precipitation frequency of the observed record and the statistics of sets from randomly generated groups of years. However, at Salt River, precipitation during El Nino occurs more frequently, and during La Nina less frequently than expected by chance. At Salt River, NDJ and especially February, March, and April (FMA) are involved - the winter rainy season is lengthened during El Nino. For Salt River heavy precipitation amounts (equal or greater than 10 $mm\,d^{-1}$) in FMA, the El Nino heavy precipitation occurs about twice as often as during La Nina.

There is some evidence that both the frequency and amount of precipitation changes during ENSO. At Yellowstone River, the NDJ El Nino vs. La Nina reduction in amount of all precipitation days is about as unusual as their El Niño vs. La Niña reduction in frequency. At Salt River, the FMA El Nino vs. La Niña increase in amount of all precipitation days is not as remarkable as their El Niño vs. La Niña increase in frequency, but clearly both phases of ENSO (El Niño and La Nina) have noticeable effects on the precipitation in both regions. 'Other years' have precipitation statistics which tend to fall in-between the El Niño and La Nina frequencies and amounts.

In NDJ, atmospheric patterns creating heavy precipitation during El Nino are very similar to those for La Niña both in interior Northwest (Yellowstone River) and in the Southwest (Salt River). However, in FMA, there is evidence that the synoptic-scale precipitation systems differ between El Nino and La Nina. The El Niño pattern shows evidence of a North Pacific basin-wide activated storm track imbedded in strong westerlies. The La Niña pattern is more confined to the eastern North Pacific and regions downstream, with a high to the west in the Gulf of Alaska vicinity and a low (often a cutoff low) along the West Coast. This same

kind of contrast appears for both Yellowstone River and for Salt River heavy FMA precipitation patterns.

It is emphasized that the daily circulation patterns shown in the composites correspond to basin average precipitation events equal or greater than 10 mm d^{-1}. Using this threshold, we have included only approximately 7% of the precipitation days at Yellowstone River and approximately 15% of the precipitation days at Salt River. The sample size of these composites ranged from 7 to 24 individual maps. As in all composites, there is a danger that there may be important differences masked by the averaging. For instance, an important issue that this analysis has not addressed is the amount of rain vs. snow, which may affect the water supply in the mountainous western United States. Since some storms within a particular group may be warm and some may be cool, further scrutiny of the cases included in each composite would be useful. Also, further tests should be performed to examine the circulation patterns associated with lighter precipitation events. Finally, since the weather during the between-storm periods is probably also a factor in the surface hydrology (via snow melt, evaporation, etc.), it would also be useful to look at differences between El Nino and La Nina dry spell weather patterns.

Flood frequency in the southwestern United States is affected by the El Niño/Southern Oscillation, but the significance of the effect varies spatially and the climatic causes are less clear. Many of the largest floods in Arizona have occurred during El Niño years. Also, certain rivers have an increased flood frequency during or within 6 mo after cessation of El Nino conditions. However, rivers strongly affected by winter storms and snowmelt may be affected more by storms that occur in years other than El Nino. This may be explained partially by lag effects after El Nino occurrence, or by floods occurring during winters with conditions of persistent, slightly negative SOI conditions that do not develop into full-fledged El Ninos, such as the winter of 1978/79.

The types of storms that generate flooding are affected by El Nino conditions, but the effects are not consistent among El Nino years. Winter storms during some El Nino years may be enhanced. Although slightly fewer tropical cyclones are generated during El Niño and La Nina years, the number of dissipating tropical cyclones that affect the southwestern United States is greatest during or following El Niño conditions. Similarly, the number of cutoff low-pressure systems affecting the southwestern United States is higher during El Nino years, but the increase is not statistically significant. The occurrence of El Nino conditions per se is not sufficient to explain increased flood frequency; instead, flood frequency may be enhanced only during a small subset of El Niño events.

Acknowledgments We thank Mike Dettinger, Henry Diaz, Art Douglas, and Katie Hirschboeck for many useful comments. We thank Editors Diaz and Markgraf for organizing the Paleoclimatic-ENSO Workshop and for encouragement and patience in seeing this manuscript through to publication. Larry Riddle and Emelia Bainto processed data, carried out analyses, and plotted results.

Marguerette Schultz drafted several figures and Jean Seifert word processed the manuscript. Part of the work by DRC was supported by the NOAA Experimental Climate Forecast Center and by the University of California Water Resources Center under Grant W-768.

References

ANDRADE, E. R. and SELLERS, W. D., 1988: El Nino and its effect on precipitation in Arizona and western New Mexico. ***Journal of Climate,*** 8: 403–410.

BARNSTON, A. G. and LIVEZEY, R. E., 1987: Classification, seasonality and persistence of low-frequency atmospheric circulation patterns. ***Monthly Weather Review,*** 115: 1083–1126.

CARLETON, A. M., CARPENTER, D. A., and WESER, P. J., 1990: Mechanisms of interannual variability of the southwest United States summer rainfall maximum. ***Journal of Climate,*** 3: 999–1015.

CAYAN, D. R. and PETERSON, D. H., 1989: The influence of North Pacific atmospheric circulation on streamflow in, the west. ***In*** Peterson, D. *H*. (ed.), ***Aspects of Climate Variability in the Pacific and the Western Americas.*** Geophysical Monograph 55. Washington, D.C.: American Geophysical Union, 375–397.

DAVIS, R. E., 1978: Predictability of sea level pressure anomalies over the North Pacific Ocean. ***Journal of Physical Oceanography,*** 8: 233–246.

DIAZ, H. F., 1991: Some characteristics of wet and dry regimes in the contiguous United States: Implications for climate change detection efforts. ***In*** Schlesinger, M. *E*. (ed.), ***Greenhouse-Gas-Induced Climatic Change: A Critical Appraisal of Simulations and Observations.*** Amsterdam: Elsevier, 269–296.

DOUGLAS. A. V. and ENGLEHART. P. J., 1981: On a statistical relationship between rainfall in the central equatorial Pacific and subsequent winter precipitation in Florida. ***Monthly Weather Review,*** 109: 2377–2382.

FU, C., DIAZ, H. F., and FLETCHER, J. O., 1986: Characteristics of the response of sea-surface temperature in the central Pacific associated with warm episodes of the Southern Oscillation. ***Monthly Weather Review,*** 114: 1716–1738.

GRAY, W. M., 1984: Atlantic seasonal hurricane frequency. Part I: El Nino and 30 mb quasi-biennial oscillation influences. ***Monthly Weather Review,*** 112: 1649–1668.

HEREFORD. R. and WEBB, R. H., in press: Historic variation in warm-season rainfall on the Colorado Plateau, U.S.A. ***Climatic Change.***

HIRSCHBOECK, K. K., 1985: Hydroclimatology of flow events in the Gila River Basin, central and southern Arizona. Ph.D. dissertation, University of Arizona, 335 pp.

HIRSCHBOECK, K. K., 1987: Hydroclimatically defined mixed distributions in partial duration flood series. ***In*** V. P. Singh (ed.), ***Hydrologic Frequency Modeling,*** Dordrecht: Reidel, 199–212.

KILADIS, G. N. and DIAZ, H. F., 1989: Global climatic anomalies associated with extremes in the Southern Oscillation. ***Journal of Climate,*** 2: 1069–1090.

KLEIN, W. H., 1957: Principal tracks and mean frequencies of cyclones and anti-cyclones in the Northern Hemisphere. U.S. Weather Bureau, Washington, D.C. ***Research Paper*** 40. 60 pp.

KLEIN, W. H. and BLOOM. H. J., 1987: Specification of monthly precipitation over the United States from the surrounding 700 mb height field. ***Monthly Weather Review,*** 115: 2118–2132.

LIVEZEY. R. E. and CHEN, W. Y., 1983: Statistical field significance and its determination by Monte-Carlo techniques. ***Monthly Weather Review,*** 111: 46–59.

LIVEZEY. R. E. and MO, K. c., 1987: Tropical-extratropical teleconnections during the northern hemisphere winter, Part II: Relationships between monthly mean northern hemisphere circulation patterns and proxies for tropical convection. ***Monthly Weather Review,*** 115: 3115–3132.

NAMIAS, J., 1981: Teleconnections of 700 mb Height Anomalies for the Northern Hemisphere. CalCOFI Atlas No. 29. Fleminger, Marine Life Research Program, Scripps Institution of Oceanography, University of California, San Diego, La Jolla, California.

NAMIAS, J., YUAN, X., and CAYAN, D. R., 1988: Persistence of North Pacific sea surface temperature and atmospheric flow patterns. ***Journal of Climate,*** 1: 682–703.

NICHOLLS, N., 1985: Predictability of interannual variations of Australian seasonal tropical cyclone activity. ***Monthly Weather Review,*** 113: 1144–1149.

PETERSON. D. H., CAYAN, D. R., and FESTA. J. F., 1986: Interannual variability in biogeochemistry of partially mixed estuaries dissolved sillate cycles in northern San Francisco Bay. ***In*** Wolfe, D. A. (ed.), ***Estuarine Variability.*** New York: Academic Press; 123–138.

QUINLAN, F. T., KARL, T. R., and WILLIAMS, C. N., JR., 1987: United States Historical Climatology Network (HCN) serial temperature and precipitation data. Prepared by T. A. Boden, Carbon Dioxide Information Analysis Center, Environmental Sciences Division, Oak Ridge National Laboratory, Oak Ridge, Tennessee.

QUINN, W. H., NEAL. V. T., and ANTUNEZ de MAYOLO, S. E., 1987: El Nino occurrences over the past four and a half centuries. ***Journal of Geophysical Research,*** 92: 14,449–14,461.

RASMUSSON, E. M. and CARPENTER, T. H., 1982: Variations in tropical sea surface temperature and surface wind fields associated with the Southern Oscillation/El Niiio. ***Monthly Weather Review,*** 110: 354–384.

REDMOND. K. and KOCH, R., 1991: ENSO vs. surface climate variability in the western United States. ***Water Resources Research,*** 27: 2381–2399.

REVELL, C. G. and COULTER, S. W., 1986: South Pacific tropical cyclones and the Southern Oscillation. ***Monthly Weather Review,*** 114: 1138–1145.

ROADS, J. O. and MAISEL, T. N., 1991: Evaluation of the National Meteorological Center's medium range forecast model precipitation forecasts. ***Weather and Forecasting,*** 6: 123–132.

ROPELEWSKI. C. F. and HALPERT, M. s., 1986: North American precipitation and temperature patterns associated with the El Niño/Southern Oscillation (ENSO). ***Monthly Weather Review,*** 114: 2352–2362.

ROPELEWSKI, C. F. and JONES, P. D., 1987: An extension of the Tahiti-Darwin Southern Oscillation index. ***Monthly Weather Review,*** 115: 2161–2165.

SCHONHER, T. and NICHOLSON, S. E., 1989: The relationship between California rainfall and ENSO events. ***Journal of Climate,*** 2: 1258–1269.

SMITH, WALTER, 1986: The effects of eastern North Pacific tropical cyclones on the southwestern United States. Salt Lake City, Utah, ***NOAA Technical Memorandum,*** NWS WR-197. 229 pp.

TRENBERTH. K. E. and PAOLINO, D. A., 1980: The northern hemisphere sea-level pressure data set trends, errors, and discontinuities. ***Monthly Weather Review,*** 108: 855–872.

U.S. Department of the Interior, Geological Survey, 1975: Index stations and selected large-river streamgaging stations in the west. ***Water Resources Review,*** p. 11.

WEBB, R. H. and BETANCOURT. J. L., 1992: Climatic variability and flood frequency of the Santa Cruz River, Pima County, Arizona. *U.S. Geological Survey, Water-Supply Paper*, 2379. 40 pp.

YARNAL, B. and DIAZ, H. F., 1986: Relationships between extremes of the Southern Oscillation and the winter climate of the Anglo-American Pacific Coast. *Journal of Climate, 6:* 197–219.